Edinburgh Research Explorer

Pleistocene terrace deposition related to tectonically controlled surface uplift: an example of the Kyrenia Range lineament in the northern part of Cyprus
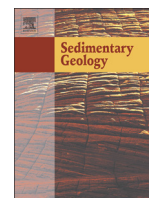
Pleistocene terrace deposition related to tectonically controlled surface uplift: An example of the Kyrenia Range lineament in the northern part of Cyprus

Romesh N. Palamakumbura, Alastair H.F. Robertson

School of GeoSciences, Grant Institute, University of Edinburgh, The King's Buildings, James Hutton Road, Edinburgh EH9 3FE, United Kingdom

A B S T R A C T

In this study, we consider how surface uplift of a narrow mountain range has interacted with glacial-related sea-level cyclicity and climatic change to produce a series of marine and non-marine terrace systems. The terrace deposits of the Kyrenia Range record rapid surface uplift of a long-lived tectonic lineament during the early Pleistocene, followed by continued surface uplift at a reduced rate during mid-late Pleistocene. Six terrace depositional systems are distinguished and correlated along the northern and southern flanks of the range, termed K0 to K5. The oldest and highest (K0 terrace system) is present only within the central part of the range. The K2–K5 terrace systems formed later, at sequentially lower levels away from the range. The earliest stage of surface uplift (K0 terrace system) comprises lacustrine carbonates interbedded with mass-flow facies (early Pleistocene?). The subsequent terrace system (K1) is made up of colluvial conglomerate and aeolian dune facies on both flanks of the range. The later terrace systems (K2 to K5) each begin with a basal marine deposit, interpreted as a marine transgression. Deltaic conglomerates prograded during inferred global interglacial stages. Overlying aeolian dune facies represent marine regressions, probably related to global glacial stages. Each terrace depositional system was uplifted and preserved, followed by subsequent deposits at progressively lower topographic levels. Climatic variation during interglacial–glacial cycles and autocyclic processes also exerted an influence on deposition, particularly on short-period fluvial and aeolian deposition.

© 2016 The Authors. Published by Elsevier B.V. This is an open access article under the CC BY license (http://creativecommons.org/licenses/by/4.0/).

1. Introduction

The combined study of shallow-marine, fluvial, and aeolian sediments can provide clear insights into the interplay of tectonics, eustatic sea-level change, and climatic change. Numerous studies have considered the allocyclic versus autocyclic controls of Pleistocene fluvial systems in the Mediterranean, for example, in southern Spain (Stokes and Mather, 2000). In addition, the tectonic versus climatic controls of Pleistocene coastal-marine and aeolian terrace deposits have been the focus of numerous studies, as in Rhodes (Titschack et al., 2005), Mallorca (Nielsen et al., 2004), and west Sardinia (Andreucci et al., 2009). However, few of these studies have shed much light on how shallow-marine, fluvial, and aeolian systems interact in response to tectonically controlled uplift during a period of eustatic sea-level change and associated climatic change.

The Pleistocene sedimentary geology of northern Cyprus provides an excellent example of how tectonically controlled surface uplift can exert a dominant control on sedimentation. Comparable studies, as in Spain (Zazo et al., 2003), west Sardinia (Andreucci et al., 2009), and Syria (Dodonov et al., 2008), have mostly focused on relatively short time periods, commonly the late Pleistocene (126 to 5 ka). However, this study provides an unusual opportunity to investigate the entire Pleistocene record in a single area of ongoing surface uplift.

The main aim of this paper is to present and discuss the results of an integrated study of successively raised marine and continental terraces, as exposed on both flanks of the Kyrenia Range in the north of Cyprus. Our specific objectives are (1) to explain the nature and distribution of the terrace deposits on the northern and southern flanks of the range based on sedimentary facies and petrographic evidence, (2) to describe and interpret the various marine and non-marine facies that are associated with each of the raised terrace deposits, (3) to evaluate different processes that have interacted to form each of the raised terrace deposits, and (4) to outline a depositional-tectonic model for terrace deposits in the light of tectonic, eustatic sea-level, and climate-related processes. Our results are potentially applicable to comparable regions of rapid surface uplift of near coastal areas elsewhere. Supporting information, including terrace correlation and geochronological data, are presented elsewhere (Palamakumbura et al., 2016a, 2016b). Specifically, field luminescence profiling has been used to help document sedimentary processes in the lowest and youngest terrace deposits (Palamakumbura et al., 2016a). Also, several types of dating have been undertaken to constrain the rate and timing of surface uplift of the Kyrenia Range (Palamakumbura et al., 2016b). The depositional

age model produced by this companion study provides a framework to help understand the sedimentary development of the raised terrace systems.

2. Influences on sedimentary development

Regions that combine coastal and fluvial terraces and which span the Pleistocene as a whole are relatively rare, and the Kyrenia Range is exceptional in this regard. The Kyrenia Range is a narrow (ca. 5 km- wide), elongate mountainous lineament, which is ca. 160 km long and up to 1024 m high (Fig. 1b). Marine and non-marine Pleistocene facies interfinger on the northern flank of the range, whereas exclusively non-marine Pleistocene deposits occur on the southern flank. Pleistocene tectonic uplift has resulted in older deposits being preserved at progressively greater heights above mean sea level (AMSL), allowing facies of different age to be distinguished without overlap. The geology of the Kyrenia Range is well known (e.g., Ducloz, 1965; Baroz, 1979; Robertson and Woodcock, l986; McCay et al., 2012), allowing detrital sediment provenance to be easily identified. A range of depositional settings, including shallow-marine, aeolian, and fluvial, is preserved within the terraces flanking the Kyrenia Range (Ducloz, 1965; Baroz, 1979). The facies on the northern flank accumulated in a setting that was open to the sea to the north, whereas those on the southern flank form part of the inter-montane (Mesaoria (Mesarya)) basin, which is itself bordered by the Troodos ophiolitic massif to the south (Fig. 1b). This allows terrace sedimentation in both marine and non-marine settings to be compared in a common tectonic setting.

Given that the terrace deposits accumulated during a period of surface uplift (Palamakumbura et al., 2016b), it is probable that tectonic processes significantly influenced their sedimentary development. In addition, the eastern Mediterranean is located at the intersection of several different climatic systems related, respectively, to continental Europe to the north (Mosbrugger et al., 2005), monsoon-influenced Asia to the east (Clift, 2006), continent-influenced North Africa to the south (Trauth et al., 2009), and the Atlantic Ocean-influenced region to the west (Ford and Golonka, 2003). The interaction of these climatic systems has had a strong influence on Pleistocene deposition in the eastern Mediterranean region (Kasse, 2002; Starkel, 2003; Cornée et al., 2012; Kober et al., 2013), including Cyprus (Waters et al., 2010; Main et al., 2016). Tectonic uplift, eustatic sea-level change, and climatic change, therefore, have to be taken into account in any interpretation of the terrace development.

3. Geological setting

The Pleistocene deposits discussed here occur extensively along both flanks of the Kyrenia Range and at its western and eastern extremities (Fig. 1b). An understanding of the pre-Pleistocene geology is critical to any interpretation of the provenance of the Pleistocene terrace deposits. The central segment of the Kyrenia Range (Fig. 1b) is dominated by Mesozoic metacarbonate rocks, whereas the eastern range is characterised by Cenozoic pelagic limestones, basic volcanic rocks, and large-scale debris-flow deposits (olistostromes). The outer flanks of the range are made up of late Eocene to late Miocene siliciclastic
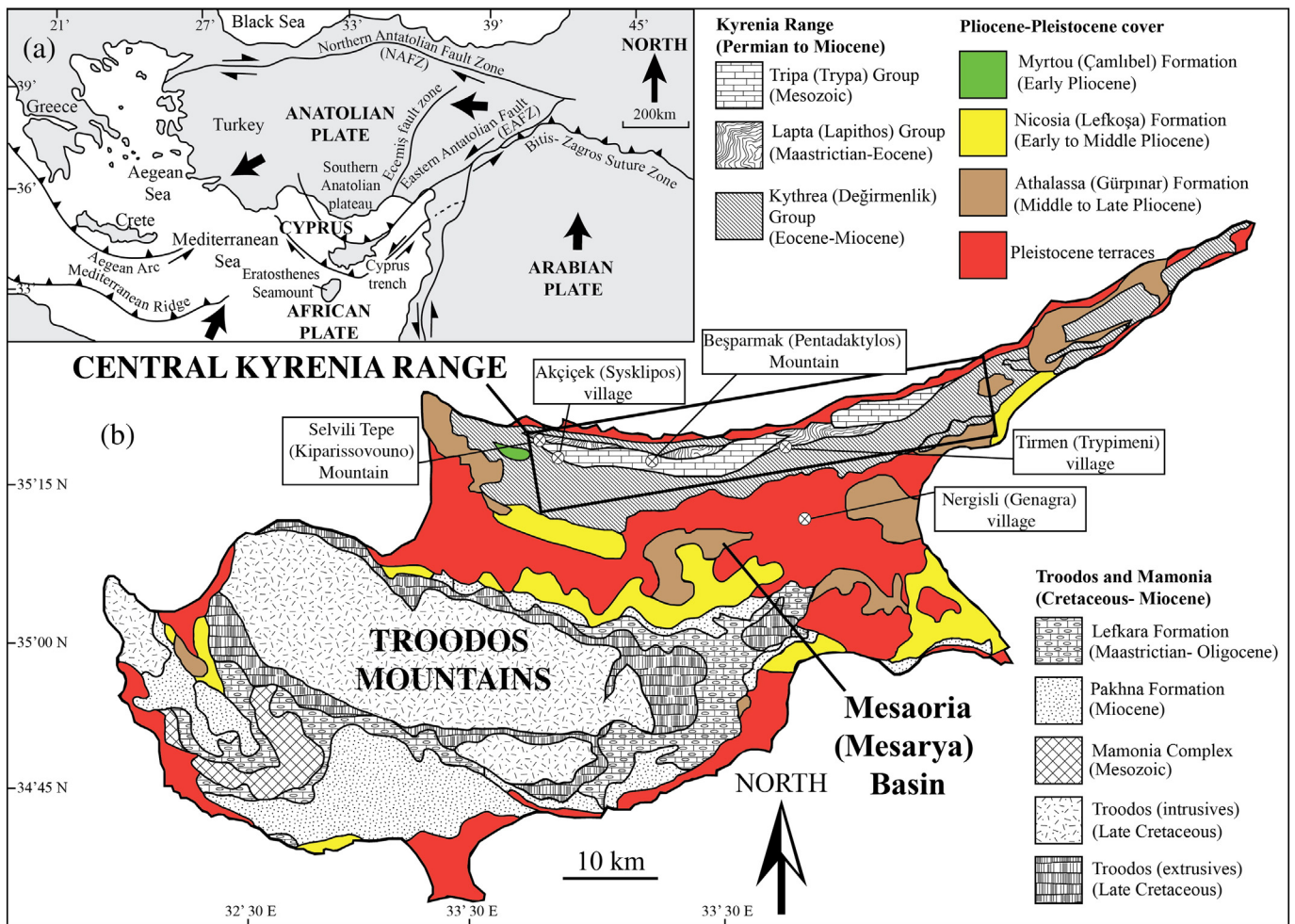

Fig. 1. (a) Summary tectonic map of the Eastern Mediterranean during the Pleistocene and (b) simplified geological map of Cyprus with emphasis on the distribution of Pliocene and Pleistocene deposits; modified after McCay et al. (2012) and McCay and Robertson (2012b).

sediments. These deposits form the substratum of most of the Pleistocene deposits. In addition, Pliocene deposits are exposed in the western, southern and eastern parts of the range.

The present work was aided by previous mapping of the Pleistocene terraces on both the northern and the southern flanks of the Kyrenia Range (Ducloz, 1964; Knup, 1965) (Table 1a, b). Early mapping indicated the existence of a series of marine and non-marine terraces on the northern flank of the range and of exclusively non-marine terraces on the southern flank of the range. The terraces were also mapped by Baroz (1979) (Table 1c), who focused on the western part of the range and established type localities for each of the main terrace deposits, based on the names of towns and villages (Table 1c). As a result, the number and the names of the terraces differed somewhat between the two main previous studies. More recently, the terraces were remapped and renamed throughout the Kyrenia Range (Hakyemez et al., 2000). In addition, a general description of the geomorphology of the Kyrenia Range was given by Dreghorn (1978). Here, we retain the previously assigned terrace names (based on Greek Cypriot names of localities and villages). More recently, introduced Turkish-language terrace names (Hakyemez et al., 2000) are included here in parentheses (Table 1).

4. Methods

During this work, the previous mapping of the terraces (Ducloz, 1964; Knup, 1965) was field checked and the terraces were correlated around both flanks of the range based mainly on height above sea level, sedimentary facies, and geomorphology. The work was carried out over three field seasons: (1) an initial three week field season during 2011 was used to follow up on the work of Ducloz (1964) and Baroz (1979), assessing their type localities; (2) the second field season of three months (2012) was undertaken to document the terrace deposits on both the northern and southern flanks of the range; and (3) a final three month field season was devoted to understanding the wider context (i.e., pre-uplift deposition) and additional terrace features. Terrace deposits, ranging from 1 to 20 m thick and up to 50 m wide, were logged at 145 localities on the northern and southern flanks of the central Kyrenia Range (Fig. 1), with the aim of understanding changes in depositional processes and settings. The terrace deposits commonly comprise several different lithologies and are generally less than 10 m thick. In general, the terrace deposits were documented on a metre scale, as this focused attention on lithological variations, facies relationships, and on changes in depositional environment.

The lower-level terraces were correlated along the northern and southern flanks of the range using a portable optically stimulated luminescence (OSL) reader. A portable OSL reader is able to make instant measurements of the luminescence properties of sediments in the field, which can be used to aid sedimentary interpretation and sampling for full OSL dating. The portable OSL reader results showed that each of

the lower terraces has a distinct luminescence signal that can be used to correlate the terraces on both the northern and the southern flanks of the range (Palamakumbura et al., 2016a). In addition, facies analysis was used to help correlate the deposits of each terrace system. In several areas, poorly preserved terrace deposits, relatively homogeneous lithofacies or karstification makes correlation difficult.

Fieldwork was supplemented by petrographical analysis of 57 sediment samples using optical microscopy. The main objective was to determine the provenance of the detrital material, including bioclastic constituents that are indicative of palaeoenvironment. Microfossils and macrofossils were identified in grainstones and conglomerates to aid interpretation of environment and climatic conditions. Terrigenous components were correlated with the pre-Pliocene geology of the Kyrenia Range to help indicate sedimentary sources and depositional pathways. The diagenetic history of the grainstone deposits was investigated using petrological analysis, focusing on the carbonate cement types. In addition, a pilot study of oxygen ($\delta^{18}O$) and carbon ($\delta^{13}C$) isotopes was carried out on seven grainstone samples, representing each of the terraces on the northern flank of the range. The isotopic analysis was carried out at the Wolfson Laboratory of the School of GeoSciences, University of Edinburgh. The analysis was carried out using a Thermo Electron Delta + Mass Spectrometer.

Dating of the terrace deposits was based on sampling the marine and aeolian deposits of the lowest terraces (Palamakumbura et al., 2016b). Samples were generally taken from the basal parts of the each terrace to determine the oldest phase of deposition in each case.

5. Occurrence and stratigraphy of terraces

The terraces were originally mapped as geomorphological features according to height above sea level (Ducloz, 1964, 1965; Baroz, 1979). In many the areas primary depositional surfaces dip seawards, such that terraces of the same age do not always occur at the same altitude. This problem was resolved by taking account of the facies and depositional relationships.

The different terrace deposits vary internally, such that we refer to them as terrace systems (Table 1d). Our recognition of the individual terrace systems makes use of a combination of (1) height above modern sea level, (2) relative heights compared to other terraces, (3) sediment facies of the terrace deposits, (4) sedimentary relationships between the terrace deposits, and (5) optical luminescence-based correlation of the lower terrace deposits (Palamakumbura et al., 2016a). This combined approach allows a revised classification and correlation of the terrace deposits on both flanks of the Kyrenia Range, as shown in Table 1d. We recognise six major raised terrace depositional systems, termed Kyrenia Range (abbreviated to 'K') terraces 0 to 5. The various components of each terrace are further subdivided based on recognition of terrace surfaces (with or without descriptions of associated deposits), and by taking account of non-marine and marine deposits. A map and

Table 1
Inferred correlations of the Pleistocene terraces in northern Cyprus, as defined by Ducloz (1964), Knup (1965) and Baroz (1979) with this study.

(a)	(b)			(c)	(d)
Ducloz (1964)	Knup (1965)			Baroz (1979)	Terrace systems (this study)
Kyrenia (Girne)	Marine		Koupia	Koupia	K5
			Kyrenia (Girne)	Kyrenia (Girne)	
Ayios Epiktitos (Çatalköy)			Ayios Epiktitos (Çatalköy)		K4
			Toumba	Agios Ermolaos (Çirinevlar)	
Toumba			Trapeza (Beşparmak)		K3
			Klepini (Arapköy)	Ayios Epiktitos (Çatalköy)	
			Kharcha II		
Trapeza (Beşparmak)	Continental		Kharcha I	Klepini (Arapköy)	K2
			Agios Iakovos (Altınova)		
Klepini (Arapköy)			Tripimeni (Tirmen)	Tripimeni (Tirmen)	K1
			Kounia		
Karka			Karka	Karka	K0
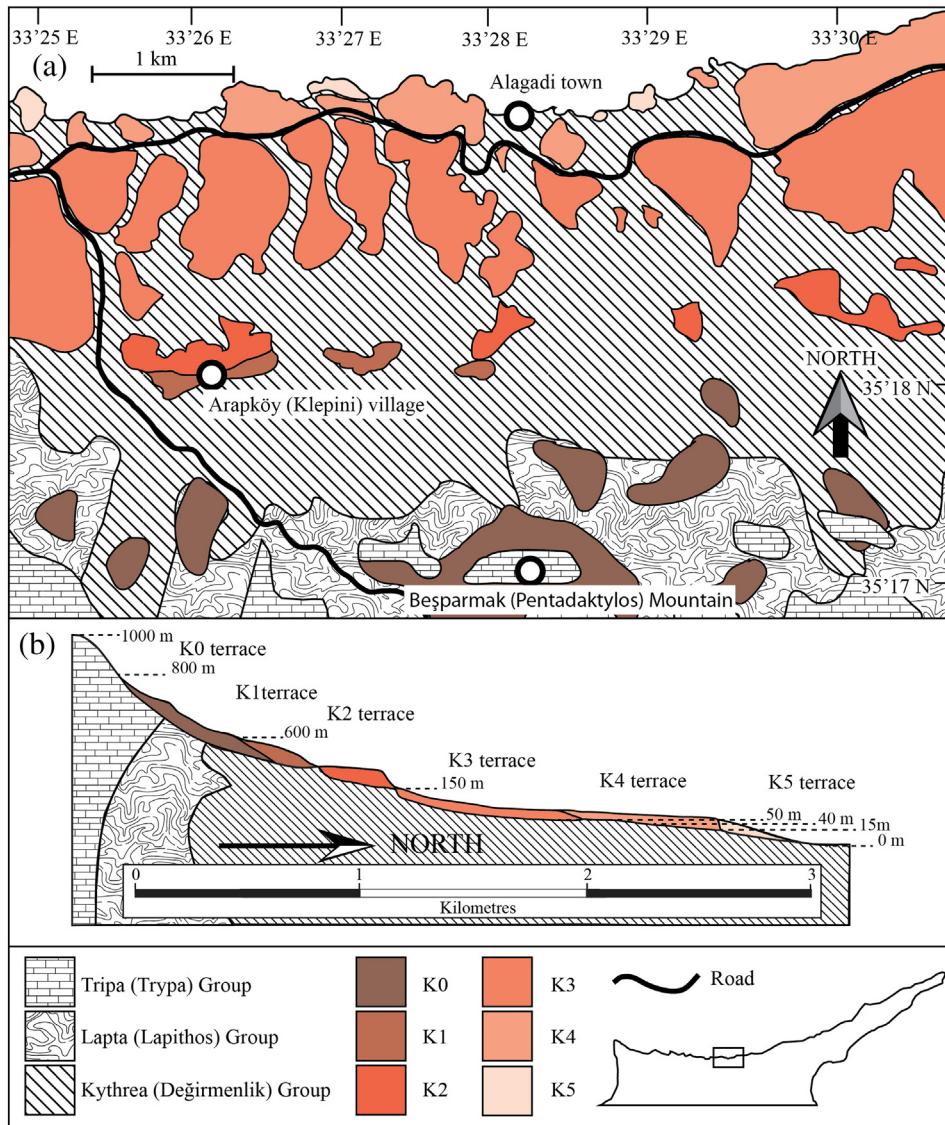
Fig. 2. (a) Geological map of part of the northern flank of the central Kyrenia Range showing the distribution of the K0 to K5 terraces (Ducloz, 1964) and (b) a simplified cross-section of the northern flank of the range showing the terrace relationships and heights.

generalised cross section of a representative part of the terrace systems along the northern flank of the central range is shown in Fig. 2.

The higher and older terrace deposits are mainly preserved as narrow fringing rims along both sides of the range, whereas the lower and younger terrace deposits are mostly exposed on gently sloping areas toward the coast in the north, and along the northern margin of the Mesaoria (Mesarya) Plain in the south (Fig. 1). As a result, in contrast to some other areas, for example, in Sicily (Pedley and Grasso, 2002), or southern Greece (Kourampas and Robertson, 2000), it is not

possible to trace depositional systems down palaeoslope for sufficient distance to allow proximal–distal facies relationships to be recognised. Largely for this reason, sequence stratigraphic analysis is not readily applicable in northern Cyprus.

The K0 to K5 terrace systems become systematically younger at lower elevations, as indicated by a combination of geomorphology, sedimentary facies relationships (see below), luminescence profiling (Palamakumbura et al., 2016a), and quantitative dating (Palamakumbura et al., 2016b). At several localities, terrace deposits

Table 2
Summary of the non-marine lacustrine facies from the highest uplifted levels of the central Kyrenia Range.

Facies	Description	Geometry	Interpretations	Terraces
A1—Chalk conglomerate (colluvium)	Matrix-supported conglomerate with subangular chalk clasts, ranging in size from 1 cm to nearly 20 cm, with occasional blocks of metacarbonate, up to 40 cm in size.	Conglomerate forms a horizontal bed ranging in thickness from 40 cm to 1.5 m. Conglomerate is preserved at the base and in the uppermost part of the deposit.	The conglomerate represents slope reworking of locally derived material into a lacustrine environment.	K0 (Karka) terrace
A2—Chalk	Fine-grained chalk with 1–3 mm-sized gastropods.	Chalk beds are ca. 50 cm thick, interbedded with the A3 facies.	Periods of high biogenic productivity within a lacustrine environment.	
A3—Mudstone	Light brown mudstone with occasional bivalve fragments.	Mudstone forms ca. 15 cm thick beds, interbedded with the A2 facies.	Periods of low biogenic activity within a lacustrine environment.	

Table 3
Summary of the facies of the K0 and K1 terrace depositional systems at the topographically highest levels of the range on the northern and southern side of the Kyrenia Range.

Facies	Description	Geometry	Interpretations	Terraces
B1—Megabreccia	Deposits range from matrix supported to clast supported. Clasts are angular, ranging in size from 1 cm to 2 m, with blocks up to 20 m. Clasts comprise metacarbonate with occasional fragments of tufa. In several localities, the deposit is covered and infilled by tufa.	Deposits range in thickness from 1 m to nearly 10 m. The breccia is thickest near metacarbonate cliffs, thinning away from these cliffs. The breccia is found at the base of metacarbonate cliffs mainly within the Kyrenia Range. Similar, deposits are absent from the eastern and western ends of the range.	Slope talus formed by fault-scarp degradation.	K0
B2—Breccia sheet	Clast-supported breccia comprising clasts that range in size from 1 to 30 cm. Clasts are subangular and elongate. The composition of the clasts is dominantly chalk.	Deposits are preserved on a series of surfaces that dip gently away from the main range. The surface width ranges from 100 to 200 m. The deposits range from 1 to 15 m thick.	Hyperconcentrated debris-flow deposits.	K0
B3—K1 colluvium	Conglomerate with subangular clasts ranging in size from 1 cm to 1 m. Clasts are composed of metacarbonate, metacarbonate breccia and reworked tufa.	The deposits are preserved proximal to the B1 breccia facies. Conglomerates are ca. 1 m thick.	Local reworking of B1 conglomerate facies.	K1

Table 4
Summary of the marine grainstone and packstone facies related to the K2 to K5 terrace systems on the northern flank of the range.

Facies	Description	Geometry	Interpretations	Terraces
C1—Well cemented grainstone	Well-cemented grainstone with numerous benthic foraminifera.	The deposit is generally <2 m thick and commonly unconformably overlies pre-Pleistocene units.	The abundant benthic foraminifera suggest an open-marine environment.	K2–K3
C2—Laminated grainstone	Fine-grained, well-cemented grainstone, with varying proportions of clastic and bioclastic material.	Parallel laminations; forms 30 to 50 cm thick units. Locally, laminated units are nearly 3 m thick.	Periods of low-energy sedimentation of reworked bioclastic and lithic material. The depositional environment was a marine-shoreface zone.	K3–K5
C3—Low-angle cross-bedded grainstone	Medium- to coarse-grained grainstone; compositionally similar to facies C2.	20–30 cm thick crossbedded units dipping at <30° in multiple directions.	Wave-dominant in a marine-shoreface environment.	K3–K5
C4—5–10 cm thick bedded packstone	Coarse-grained, lithic and bioclast-rich packstone. Clastic material is mainly metacarbonate; bioclastic material is reworked mollusc shells. Locally within these beds there are rip-up clasts of basal lithologies or older lithified grainstones.	5–10 cm-thick beds with well-developed normal grading.	Shoreface environment with high-energy current reworking of lithic and bioclastic material; likely to represent short-lived storm events.	K4
C5—Gastropod-rich packstone	Packstone comprising >90% gastropod shells, 0.5–1 cm sized.	5–10 cm thick beds that are well sorted, lacking sedimentary grading.	Shallowing into a low energy, stressed environment, such as a coastal lagoon.	K4

Table 5
Summary of the marine conglomerate facies from the K2 to K5 terrace systems on the northern flank of the range.

Facies	Description	Geometry	Interpretations	Terraces
D1—Grainstone breccia	Breccia clast size ranges from 1 cm to nearly 2 m. The clasts are dominantly well-cemented grainstone. The grainstone clasts contain well-preserved corals, molluscs and serpulid worm tubes. The clasts are generally elongate.	Deposits are ca. 1 m thick (2 m-sized clasts are elongate and orientated parallel to bedding). The deposits form horizontally continuous beds within the F7 facies.	Marine transgression of a deltaic system resulting in decreased clastic input and the development of a shallow-marine fauna including solitary corals.	K4
D2—Conglomerate with reworked clastic and bioclastic material.	Conglomerate clasts are composed of reworked grainstone and packstone, metacarbonate, chalk, chert, and basalt. The deposits have a medium-grained to coarse-grained, well-lithified carbonate sand matrix. Clasts range from 1 to 30 cm and are subrounded to well-rounded.	Deposit forms 30 to 50 cm thick beds within the lower parts of the C2, C3 and C4 grainstone facies.	Storm deposits reworking lithified grainstone and inputting clastic material from onshore.	K4–K5
D3—Conglomerate made up of well-rounded clastic and *in situ* biogenic material.	Conglomerate ranging from clast to matrix supported; composed of well-rounded lithic and biogenic material. The lithic material includes metacarbonate rock, mudstone, chert, diabase, and serpentinite. The biogenic material includes: *in situ* coral, pectens, oysters, gastropods, calcareous algae, and serpulid worm tubes.	Conglomerate forms laterally continuous beds, ranging from 2 to 5 m long. The deposit ranges in thickness from 30 cm to 1 m. Interbedded with marl facies.	Shallow-marine environment with intermittent clastic input. Shallow-marine fauna developed in a low-energy environment and were locally reworked by high-energy flows.	K4
D4—Conglomerate with well-rounded clasts.	Clast-supported conglomerate with well-rounded, imbricated clasts. Clasts ranging from 1 to 10 cm and are well sorted. The clasts are compositionally similar to those in the D3 facies.	Conglomerate comprises 20–30 cm thick parallel beds. The conglomerate is generally interbedded with E1 and E3 aeolian grainstone facies.	Pebble beach environment	K4

Table 6
Summary of the aeolian grainstone facies from the K2 to K5 terrace systems on the northern flank of the range.

Facies	Description	Geometry	Interpretations	Terraces
E1—High-angle planar cross-bedded grainstone	Well-sorted, fine- to medium-grained grainstone. (The composition of the grains is the same as in the C2 facies). Calcified palaeo-root traces are preserved in the upper part of the deposit.	1–2 m thick planar cross-bedded units, separated by 30 cm-thick units of laminated grainstone. The palaeoflow direction of the cross bedding is either toward the west or the east (parallel to the coast).	Onshore dune field with a palaeowind direction parallel to the coast.	K1–K4
E2—1–3 m thick trough cross-bedded grainstone	Medium- to fine-grained grainstone. Calcified palaeo-root traces are commonly preserved throughout the deposit. The grains are dominantly composed of lithic material plus a minor amount of bioclastic material.	1–3 m thick trough cross-bedding with forests dipping from 20 to 40°. The palaeoflow direction varies significantly within and between the deposits.	Onshore dune field with multiple palaeowind directions. The deposit represents multiple phases of deposition that allowed vegetation to develop.	K5

are observed to truncate and overlie topographically higher terrace deposits. Also, the relative age relationships implied by uranium disequilibria isotopic dating and OSL dating confirm that the K4 terrace predates the K5 terrace (Palamakumbura et al., 2016b).

The K0 terrace, which is equivalent to the traditional Karka terrace (Ducloz, 1972) (Table 1), is mainly preserved within the central Kyrenia Range (Fig. 2). This terrace ranges from ca. 600 to 800 m AMSL (Fig. 2b) and can be correlated as a single depositional system along the northern and southern flanks of the range. The K0 terrace is made up of megabreccia, debris-flow and lacustrine deposits. At several localities, the megabreccias of this terrace system are underlain by fine-grained calcareous sediments that include coarse clastic intercalations. Lacustrine deposits are preserved within small intramontane basins, tens to hundreds of metres across by up to several kilometres long. Although generally obscured by younger deposits, wells drilled into several of these small basins have revealed lacustrine deposits up to 5 m thick (Ducloz, 1972).

The K1 terrace system is dominated by non-marine conglomerates, which are discontinuously exposed along the northern and southern flanks of the range from ca. 300 to 600 m AMSL (Fig. 2). The K1 terrace surface is continuous with the K0 surface, dipping gently away from the range on both its northern and southern flanks. The K1 surface is heavily dissected by fluvial erosion resulting in 50 to 200 m-wide, discontinuous surfaces.

The K2 terrace system is characterized by a discontinuous upper surface that trends east–west, subparallel to the range at between 140 and 180 m AMSL on the northern flank, and ca. 300 to 400 m AMSL on the southern flank (Fig. 2). The K2 terrace system is <500 m to ca. 2 km wide.

The K3 terrace system shows a significant variation in height above mean sea level, from nearly 150 m down to ca. 40 m AMSL (Fig. 2). The K3 terrace forms a northward-dipping surface between the K2 and K4 terraces (Fig. 2b), which results in up to ca. 100 m variation in the height of the terrace deposits of the same depositional system. The K3 terrace surface is ca. 100 m below the base of the K2 terrace on both flanks of the range (Fig. 2b).

The K4 terrace surface is extensively, but discontinuously, exposed on both the northern and southern flanks (Fig. 2). The terrace surface ranges from 1 to 2 km wide and runs subparallel to the range. The K4 terrace deposits vary from 5 to 40 m AMSL on the northern flank of the range but are as high as ca. 100 m AMSL on the southern flank.

Table 7
Summary of the fluvial facies related to the K2 to K5 terrace systems on the northern and southern flanks of the range.

Facies	Description	Geometry	Interpretations	Terraces
F1—Fine-grained mudstone	Fine-grained to medium-grained mudstone	Massive and structureless deposit	Low-energy deposition within a fluvial environment.	K2–K5
F2—Clast-supported conglomerate (<40 cm thick lenses)	Conglomerate with subangular clasts, ranging in size from 1 to 20 cm. Clasts are moderately to well-sorted within lenticular shaped beds. The clasts are mainly metacarbonate rock but include chalk, basalt, chert, metacarbonate breccia, sandstone and mudstone.	Conglomerate forms lenticular-shaped beds within the mudstone. Lenses range in size from 10 to 40 cm thick and from 1 m to nearly 10 m long. Poorly developed normal grading is commonly observed.	Conglomerate channels representing pulses of deposition during debris-flow events.	K2–K5
F3—Clast-supported conglomerate (>1 m thick lenses)	Clasts within the conglomerate range in size from 1 to 40 cm and are subangular to angular. The clasts are compositionally the same as the F2 facies (above).	Conglomerate within lenticular-shaped beds that are 1–2 m thick and 2–4 m long. Lenses are made up of 10–30 cm-thick beds that are moderately to well sorted.	High-energy debris flows are associated with major incision within a fluvial depositional environment.	K2–K4
F4—Bedded conglomerate (alluvium)	Conglomerate clasts are subangular to well-rounded, well-sorted and range in size from 1 to 20 cm. The composition of the clasts is the same as in the F2 facies.	Conglomerate deposits form continuous beds ranging in thickness from 30 cm to 1 m. Beds are well sorted and have well preserved normal grading.	High-energy perennial streams.	K2–K5
F5—Conglomerate (colluvium)	Conglomerate containing subangular clasts ranging in size from 1 to 40 cm. The clasts comprise chalk, chert, basalt, serpentinite and metacarbonate rock.	Conglomerate deposit ranging in thickness from 1 m to nearly 3 m thick. Clasts are poorly sorted and lack sedimentary organization.	Reworking of conglomerate downslope within a fluvial drainage system.	K2–K5
F6—Palaeosol	Fine-grained palaeosol ranging in colour from dark-maroon to red. Caliche is preserved in several horizons.	Palaeosols forming horizontal beds within mudstone and conglomerate.	Preserved soil horizons represent a period of landscape stability during warm humid climate with relatively low fluvial run-off.	K2–K4
F7—Cross-bedded gravel	Conglomerate with clasts ranging in size from 1 to 5 cm. The beds within the conglomerate are well sorted. Clasts are subrounded to well-rounded. Clasts are dominantly metacarbonate of the Tripa (Trypa) Group.	Low-angle, 30–50 cm thick, cross-bedded units. Occasional outsized clasts range in size from 10 to 30 cm.	Gilbert-type deltaic environment, representing periods of increased fluvial run-off.	K4
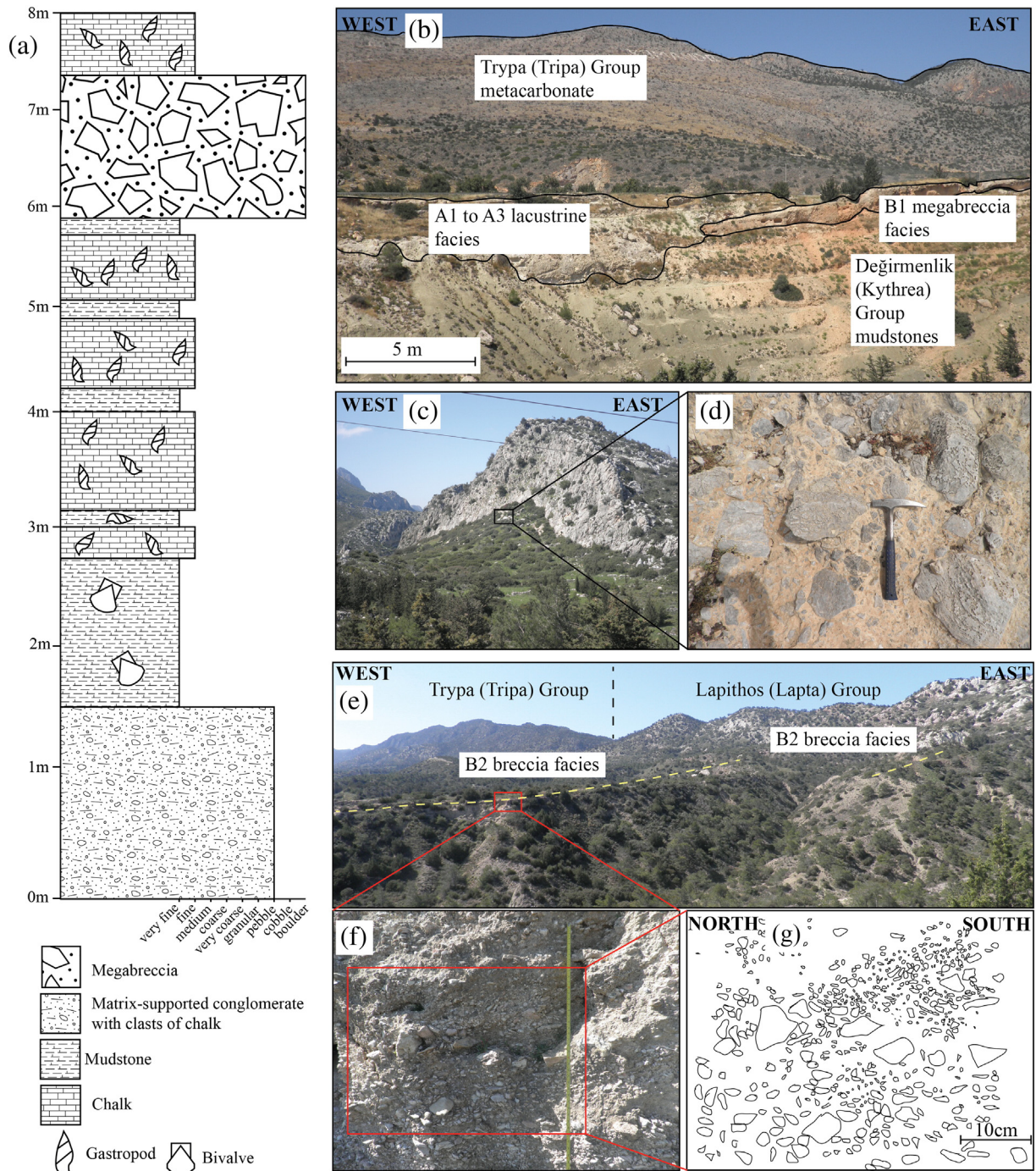
Fig. 3. Photographs and sketches of deposits of the K0 terrace system: (a) Summary log of the lacustrine facies (A1–A3 facies) preserved in the central Kyrenia Range; (b) labelled photograph of the interbedded relationship of the lacustrine facies and B1 facies megabreccia; (c) photograph of the K0 terrace megabreccia at the base of a metacarbonate-rock cliff; (d) photograph of the B1 facies megabreccia of the K0 terrace; (e) photograph of the B2 breccia deposit surface dipping away from the E-W axis of the Kyrenia Range; (f) photograph of the B2 facies breccia; (g) sketch of the B2 facies breccia.

The K5 terrace system is preserved very near the northern coast (Fig. 2) and also within the Mesaoria (Mesarya) Basin to the south of the Kyrenia Range (Fig. 1). The K5 terrace surface runs discontinuously parallel to the range on the northern flank at <20 m AMSL. On the southern side, the equivalent surface is exposed within the central part of the Mesaoria (Mesarya) Plain (Fig. 1). The K5 terrace deposits are very near mean sea level on the northern flank of the range and at ca. 50 m AMSL within the Mesaoria (Mesarya) Plain.

In summary, the upper terraces (K0 and K1) on both the northern and southern flanks of the range are between 600 and 300 m AMSL. In contrast, the lower terrace surfaces and deposits (K2 to K5) on the southern flank of the range are generally higher above mean sea level than the equivalent terraces on the northern flank of the range. This difference in height can be explained by the contrasting depositional-tectonic settings of the two range flanks. The northern flank was open to the Mediterranean Sea allowing easy sediment bypassing, whereas
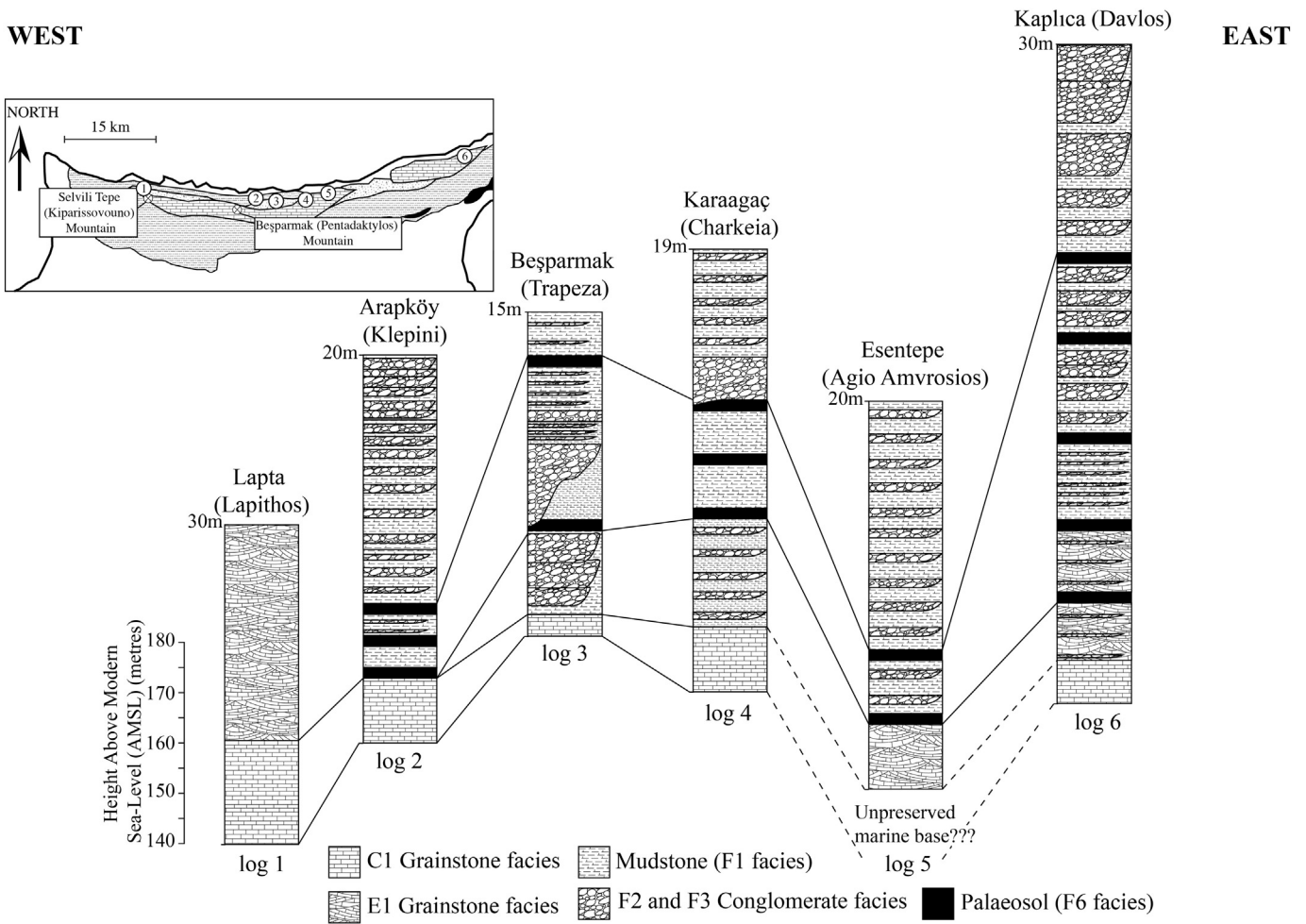
Fig. 4. Summary logs of the K2 terrace system deposits on the northern flank of the Kyrenia Range, with heights above modern sea-level from the base of each section (as shown by the scale of the left); the deposit thickness is labelled on each log.

the southern flank borders the intermontane Mesaoria (Mesarya) Basin, which captured a relatively greater volume of erosional detritus.

6. Facies associations

The deposits associated with the different terrace systems have many features in common, although some are distinctive to specific terraces or areas. To avoid duplication, the facies are summarised below as a whole, with reference to the terrace systems in which they occur, with unusual features being highlighted. We recognise a series of facies associations, which correspond to the various depositional environments observed within the K0 to K5 terrace systems, as follows: Facies association A, lacustrine (Table 2); Facies association B, megabreccia and debris-flow deposits (Table 3); Facies association C, marine grainstone and packstone (Table 4); Facies association D, marine conglomerate (Table 5); Facies association E, aeolian grainstone (Table 6); and Facies association F, fluvial (Table 7). For each of these facies associations (labelled arbitrarily A-F), a series of specific facies is defined, as summarised in Tables 2–7. The facies descriptions are followed by an interpretation of the relevant palaeoenvironments. The contributing sedimentary processes are then discussed. To supplement this analysis we present representative logs from the raised terraces on the northern flank of the range, focusing on various well-preserved facies relationships (Figs. 3–6). Poorly exposed sections are not shown as logs but are included in the facies analysis. Sedimentary logs are not given from the southern flank of the range because all of the observed fluvial

facies also occur on the northern flank. However, sedimentological information from the southern flank is included in the overall interpretation.

6.1. Facies association A: fine to coarse-grained and conglomeratic non-marine calcareous facies

The highest-level terrace (K0) on both flanks of the range (Table 2) encompasses two related deposits, where locally exposed. In a few relatively small (several square kilometres) areas of the central range, fine-grained calcareous sediments are exposed at the base of the K0 terrace, together with very coarse clastic intercalations (Fig. 3a, b). This type of sequence was previously treated as part of the Karka terrace (Table 1a-c) of the Fanglomerate Formation (Ducloz, 1972; Baroz, 1979). However, the lithologies differ greatly from the very coarse clastic material that characterises the K0 terrace system as a whole.

The various fine-grained lithologies are defined as facies A1 to A3 (Table 2). The A1 facies is poorly sorted conglomerate, comprising angular clasts, predominantly chalk and also rare metacarbonate rock. The A2 facies is fine-grained chalk with occasional mollusc and ostracod fragments (1–3 cm sized). The A3 facies is fine-grained, light-brown mudstone that also contains similar fossil fragments. The main part of the deposit is formed of interbeds of A2 facies (chalk) and A3 facies (mudstone), up to 7 m thick. The A1 facies conglomerate is exposed near the base and near the top of the sequence. The uppermost levels of the sequence are locally intercalated with megabreccia of the K0
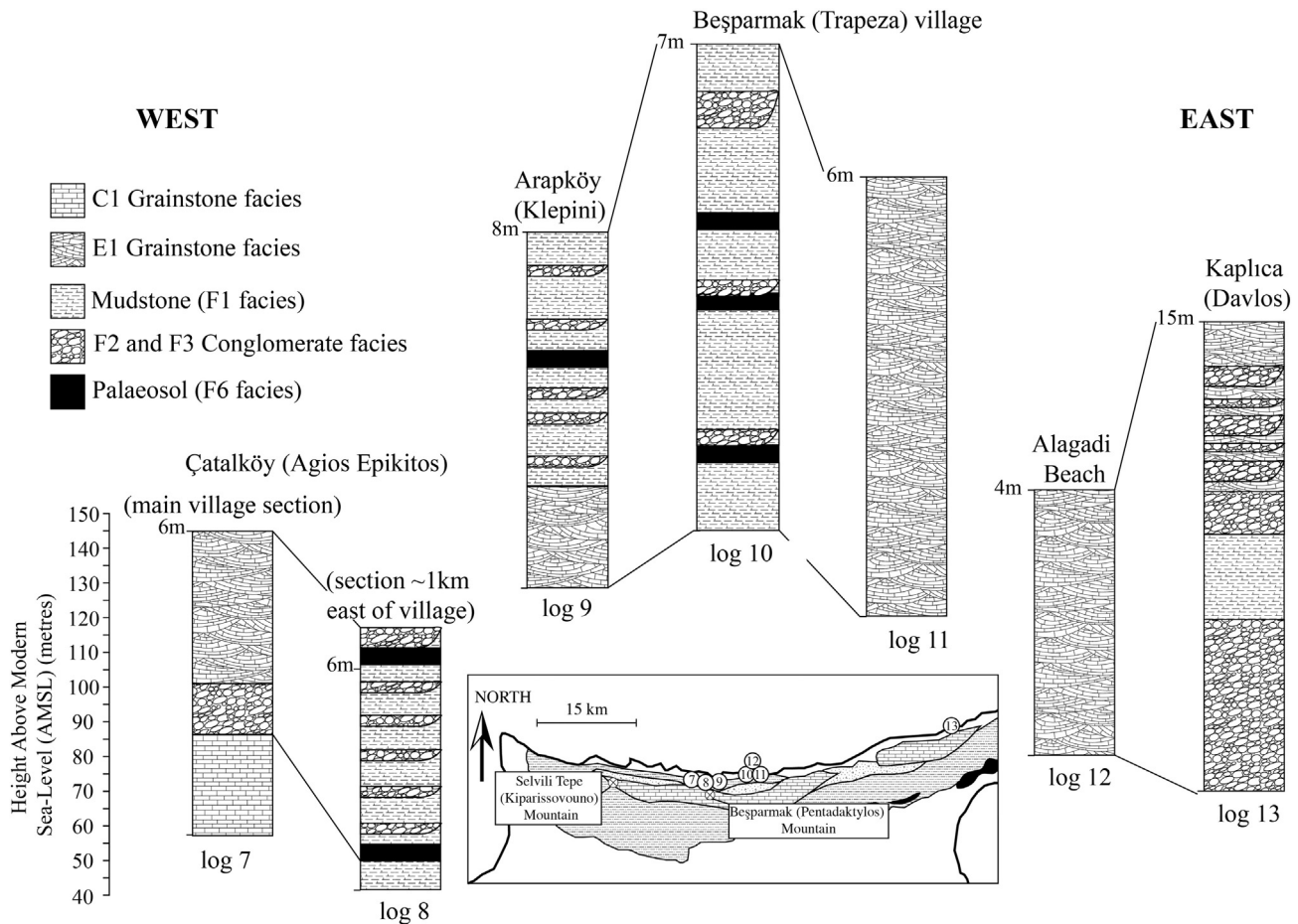
Fig. 5. Summary logs of the K3 terrace system deposits on the northern flank of the Kyrenia Range, with heights above modern sea level from the base of each section (as shown by the scale of the left); the deposit thickness is labelled on each log.

terrace (Fig. 3b). The molluscs *Planorbis carinatus*, *Valvata pisceinalis*, *Limnaea ovata*, and *Pisidium nitidum* are observed in both the A2 and the A3 facies and are indicative of a non-marine environment (Ducloz, 1972).

6.2. Interpretation: localised lacustrine facies

The interbedded A2 and A3 facies represent a low-energy environment, as indicated by their fine-grained nature and lack of current-flow structures. The thin-shelled gastropods and ostracods lived in a freshwater, lacustrine environment (Ducloz, 1972). The A1 facies conglomerates show little signs of sedimentary sorting during transport and are interpreted as locally reworked colluvium (slope-wash material). The observed chalk and mudstone facies are similar to deposits within the Fucino Basin of central Italy (Cavinato et al., 2002) and Lake Bonneville in northern Utah, USA (Lemons and Chan, 1999), although the scales of these deposits differ from counterparts in the Kyrenia Range.

### 6.3. Facies association B: megabreccias and debris-flow deposits

The highest-level K0 terrace is made up of several different breccia facies (Table 3), which are well exposed at Beşparmak (Pentadaktylos) Mountain (Figs. 2a, 3c, d).

The dominant facies is the B1 facies megabreccia (Table 3). The prefix "mega" describes conglomerate that contains clasts that are 4.1 to 65.5 m in size, based on the Udden-Wentworth classification (Wentworth, 1922; Blair and McPherson, 1999). The megabreccia (B1

facies) comprises angular clasts of Mesozoic metacarbonate rocks (Fig. 3d), which range from 1 cm to 20 m in size. The megabreccia is commonly matrix supported, although a clast-supported fabric appears in sections that are over ca. l km away from the range in some areas. The matrix, where present, is well-cemented, fine-grained mudstone. Tufa (cool-water carbonate) occurs extensively on surfaces and within spaces between blocks in the megabreccia. Owing to erosion or covering by young talus, the B1 facies varies from very well preserved in some areas (e.g., Selvili Tepe (Kiparissovouno Mountain)), to poorly preserved, or absent in others (e.g., Tirman (Trypimeni)) (see Fig. 1).

The megabreccias are commonly preserved at the base of cliffs and very steep slopes that have been eroded into Mesozoic metacarbonate rocks (Trypa (Tripa) Group) (Fig. 3c). Where exposed, the substratum of the megabreccias is commonly weathered Neogene siliciclastic sedimentary rocks (Kythrea (Değirmenlik) Group (Weiler, 1970; McCay and Robertson, 2012a), for example, around Akçiçek (Sysklipos) village (Fig. 1). In places, the megabreccias extend up to ca. 500 m downslope from exposed cliffs.

Cobble-sized breccias (B2 facies; Table 3), 1 to 15 m thick, are commonly present within the central range, where the basement is mostly dominated by latest Cretaceous to Palaeogene pelagic carbonate and basaltic lava (Lapithos (Lapta) Group); e.g., near Tirmen (Trypimeni) village (Fig. 1b). The breccias are capped by geomorphologic surfaces (100–200 m wide) that dip gently away from both flanks of the central range (Fig. 3e). The breccias are dominated by angular to bladed clasts that range from 1 to 30 cm in size and exhibit normal size grading (Fig. 3f, g). The deposits as a whole are clast supported with a volumetrically minor, fine-grained, pink marly matrix. Poorly developed clast
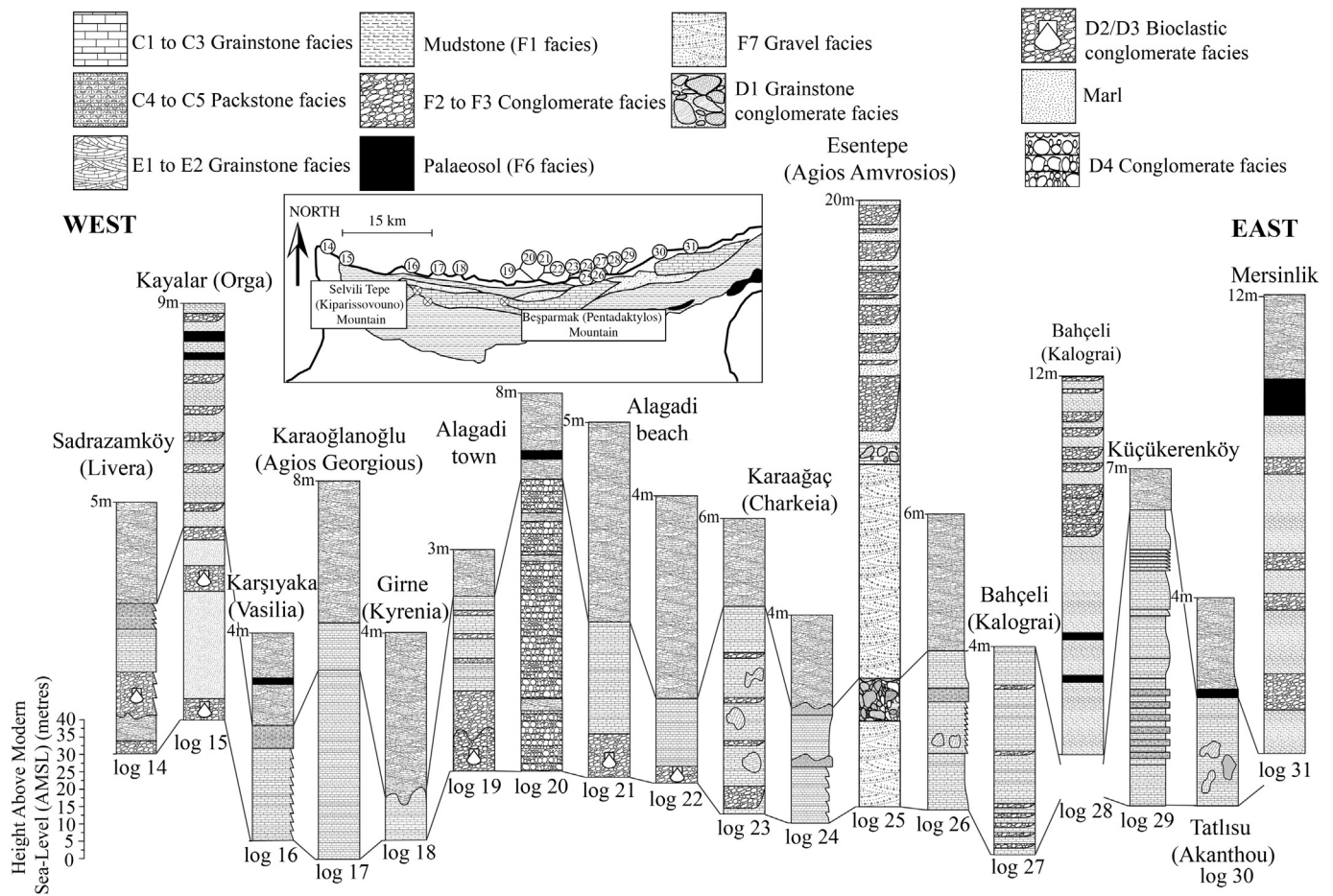
Fig. 6. Summary logs of the K4 terrace system deposits on the northern flank of the Kyrenia Range, with heights above modern sea level from the base of each section (as shown by the scale of the left); the deposit thickness is labelled on each log.

imbrication indicates palaeoflow away from the range. In several exposures, discontinuous beds (ca. 5 cm thick) of conglomerate include well-sorted clasts with well-developed normal grading.

Commonly associated with the B1 facies megabreccia deposit is the B3 conglomerate facies (Table 3). This is preserved discontinuously on both the northern and southern flanks of the range. The deposits are mostly <1 m thick by 10 m in lateral extent and lack sedimentary sorting. This facies is made up of subangular to subrounded clasts of metacarbonate rocks (1 cm–1 m in size), together with fragments of lithified B1 facies megabreccia and detrital tufa.

6.4. Interpretation: mass-wasting deposits

The B1 facies megabreccia is interpreted as the result of the collapse and mass wasting of very steep slopes that are dominated by Mesozoic metacarbonate rocks. Reworked tufa clasts observed within the B2 colluvium facies indicate that some tufa formed during the earliest stage of B1 megabreccia deposition. Tufa formation is likely to have been ongoing owing to the large amounts of tufa observed within the deposit and on the surface of the B1 megabreccia. This facies is, for example, similar to the slope-talus facies of the Rocca Busambra ridge in western Sicily (Basilone, 2009). The B2 conglomerate facies is inferred to represent a hyperconcentrated flow deposit (Coussot and Meunier, 1996) that resulted from short-lived, repeated, high-energy depositional events. The predominantly carbonate and volcanic clasts were sourced from 'basement' exposures <1 km away from the range axis. In addition, the B3 facies conglomerate is interpreted as the product of slope wasting (i.e., colluvium), as suggested by a combination of matrix-supported clasts, local clast derivation and an absence of sorting, similar

for example, to deposits described from west-central Anatolia (Nemec and Kazanci, 1999).

6.5. Facies association C–D: carbonate and conglomerate marine deposits

On the northern flank of the range, a major component of the terrace systems is represented by several different facies of grainstone, packstone, conglomerate, and breccia, which unconformably overlie mudstones and sandstones of the Kythrea (Değirmenlik) Group. The marine deposits include C1 to C5 facies grainstone and packstone (Table 4) and also the D1 to D4 facies marine conglomerate and breccia (Table 5).

The C1 facies grainstone is well cemented and comprises well-rounded grains, predominantly comprising the benthic foraminifera *Miliolida*. This facies is preserved as <2 m-thick depositional units within the uppermost terraces (K2 and K3) (Fig. 4 logs 1–4; Fig. 5, log 7). Rare, poorly preserved planktonic foraminifera were observed within this facies during this work. The C2 grainstone facies (Table 4) forms 30 to 50 cm-thick, fine- to medium-grained depositional units, with well-preserved parallel lamination. The C3 grainstone facies (Table 4) is medium to coarse grained, with well-preserved, low-angle (<30°) cross bedding. The C2 and C3 facies grainstones are interbedded, forming 1 to 5 m-thick deposits (e.g., Fig. 6, logs 16, 17, 29). The C4 facies packstone (Table 4) is made up of coarse bioclastic and siliciclastic grains, ca. 0.5 cm in size, which vary from well-rounded to angular. Individual beds (5–10 cm thick) exhibit well-developed normal grading. Clasts of underlying bedrock (e.g., packstone and mudstone) are locally present. The bioclastic material is made up of mollusc shells and reworked coral. The C5 packstone (Table 4) is exclusively made up of

mollusc shells, predominately gastropods, together with occasional bivalves. The C5 facies (Table 4) forms 5 to 10 cm thick beds, which are laterally continuous for up to 5 m. The C4 and C5 facies packstones occur as interbeds within the C2 and C3 facies grainstone of the K4 terrace system (Fig. 6, logs 24, 26, 29). Marine conglomerate facies are interbedded with the grainstone facies (Table 5; Fig. 6, logs 14, 19, 30) and with the F7 gravel facies (Table 7; Fig. 6, log 25).

The D1 facies conglomerate (Table 5) comprises disorganised, angular blocks of well-cemented grainstone, from 1 cm to ca. 2 m in size. Well-preserved solitary coral, bivalves, serpulid worm tubes, and bored shells characterise this facies. The deposit is clast supported with <10% matrix, largely composed of unlithified sand (Fig. 6, log 25).

The D2 facies conglomerate (Table 5) comprises mixtures of detrital clastic and bioclastic material. The detrital material is reworked carbonate grainstone and packstone, metacarbonate rock (limestone and dolomite), chalk, chert, and basalt. The bioclastic material comprises fragmented solitary corals (*Cladacora caespitosa*), bivalves, gastropods, and serpulid worm tubes. The clasts range in size from 1 to 30 cm and vary from subangular to well-rounded. The deposit varies from 30 to 50 cm in thickness and is interbedded with the D2 and D3 facies grainstone (Fig. 6, logs 15, 21, 29).

The D3 facies conglomerate (Table 5) comprises well-rounded lithic clasts (1–10 cm in size), together with *in situ* biogenic material (preserved at ca. 40 m AMSL). The detrital material is mostly metacarbonate rock, mudstone, chert, diabase, and serpentinite. Biogenic material was mainly derived from solitary coral (*C. caespitosa*), bivalves (including *Spondylus* sp. and *Glycymeris* sp.), gastropods, calcareous algae, and serpulid worm tubes. The fragments range from 1 to 10 cm in size. The conglomerate is clast supported with a matrix of unlithified mud (<20% by volume). The deposit forms 30 cm to 1 m-thick beds within grey to brown marl. The combined interbedded conglomerate and marl is ca. 4 m thick (Fig. 6, log 15).

The D4 facies conglomerate (Table 5) is made of well-rounded and well-sorted clasts, ranging from 1 to 10 cm in size (located at ca. 20 m AMSL). The clasts comprise metacarbonate, sandstone, mudstone, serpentinite, and chert and are organised into parallel beds, 20 to 30 cm thick, with well-developed normal grading. In addition, well-developed westward-directed clast imbrication is locally observed. Poorly lithified E2 facies grainstones occur as lenses or as continuous beds up to 10 m thick (Table 6; Fig. 6, log 20).

6.6. Grainstone composition

The most common bioclasts in both the marine and the non-marine grainstones are echinoderm plates and calcareous red algae (Fig. 7a, b). Common benthic foraminifera include *Miliolida* and *Neorotalia*, plus occasional *Peneroplidae* and *Textulariidae* (Fig. 7c–f). Variable amounts of bivalve shell fragments, notably pectens and oysters (e.g., *Gryphaea* sp.) (Fig. 7g, h) are also present. There are also reworked fragments of serpulid worm tubes and calcareous algae (Fig. 7i, j), bryozoa, ostracods, gastropods, and planktonic foraminifera. Siliciclastic material is mostly monocrystalline quartz, polycrystalline quartz, plagioclase, chert, and diabase (Fig. 8a–e). Reworked carbonate rocks include metacarbonate, grainstone, and foraminifera-rich marl (Fig. 8f–h). The relative proportions of carbonate and siliciclastic grains vary significantly between the grainstone facies in different areas. Biogenic grains are heavily fragmented and rarely preserved as intact fossils. In addition, the clastic grains range from subangular (Fig. 8a) to well rounded (Fig. 8f–h). The C1–C3 and E1–E2 grainstones mostly have a finely crystalline sparite cement (<50 μm), which coats grains (rim cement) and partially, to completely, infills pore spaces (Fig. 7a–i). The amount by which the pore space is infilled varies from ca. 10% to 100% in different grainstone deposits. Several of the grainstones contain both micritic and sparite cements, with the micritic cements coating grains, and the sparite cement infilling interstitial spaces. The C2–C3 grainstone facies rarely has a

micritic pore-filling cement with no sparite cement preserved. However, no variation in cement type is observed between the C1–C3 and E1–E2 grainstone facies. Preliminary $\delta^{18}O$ and $\delta^{13}C$ data were obtained from the carbonate cements of C2 and E2 grainstone facies and have $\delta^{18}O$ values of −3.03 to −4.52 and $\delta^{13}C$ values of −3.63 to −7.07 (Palamakumbura, 2015).

6.7. Interpretation: shallow-marine carbonate deposition

The C1 to C5 and the D1 to D4 facies represent coastal, to shallow-marine depositional environments, which are preserved along the northern flank of the Kyrenia Range.
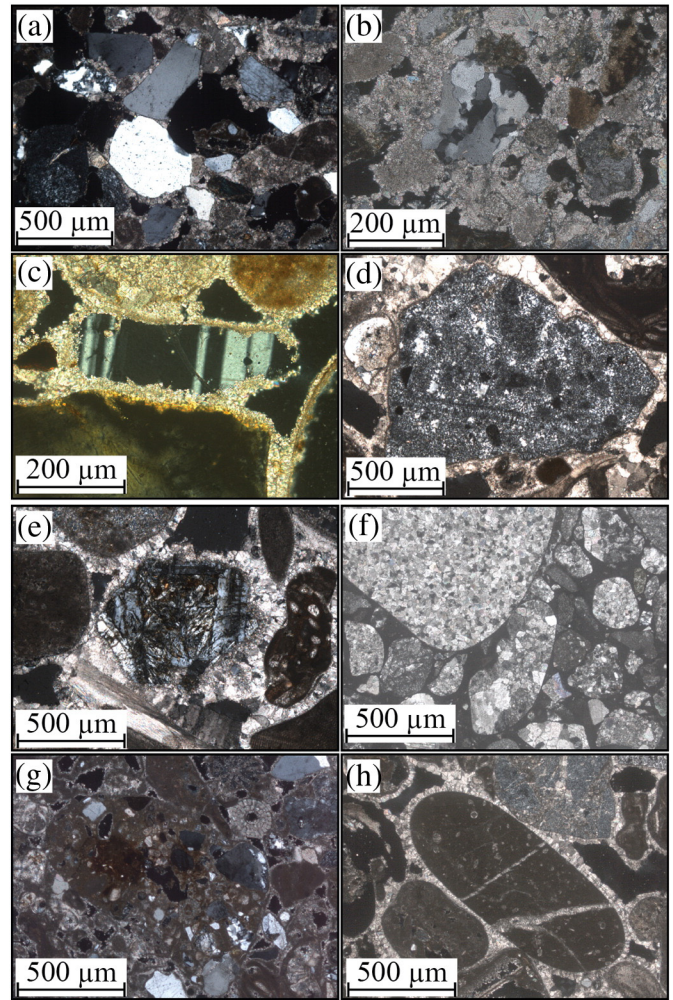
The C1 grainstone facies records a relatively low-energy, open-marine, offshore environment, characterised by abundant benthic foraminifera. Rare planktonic foraminifera were mostly reworked from older deposits. The reworked planktonic foraminifera are mostly broken or abraded and include (or are attached to) remnants of pre-existing sediment. In contrast, contemporaneous planktonic foraminifera are well preserved as intact tests, either without internal carbonate cement or with cement fabrics similar to the enclosing sediment. Similar grainstone facies have been widely reported from the Mediterranean and elsewhere (e.g., Pedley and Grasso, 2002; Pedley and Carannante, 2006; Cornée et al., 2012). The interbedded C2 and C3 facies are again interpreted as shallow-marine deposits with abundant bioclastic material, including benthic foraminifera, calcareous red algae, bryozoa, and ostracods. The parallel-laminated C2 facies represent deposition due to sediment settling from the water column, and is interpreted as a low-energy marine deposit. In contrast, the presence of well-preserved low-angle, multidirectional cross bedding suggests that the C3 facies is wave controlled (Burchette and Wright, 1992). The interbedded C2 and C3 facies reflect variations in wave energy in a shoreface environment within a shallow-marine setting (Clifton et al., 1973; Pedley and Grasso, 2002). The reworked grains of calcareous red algae, echinoderms and benthic foraminifera within the C2 and the C3 grainstone facies were sourced from a littoral-marine environment. Based on normal grading and the presence of rip-up clasts, the C4 facies packstone is interpreted as a tempestite, similar to examples described from Israel (Buchbinder and Zilberman, 1997) and Rhodes in Greece (Hansen, 1999). The C5 facies packstone is interpreted as representing a low-energy backshore, to lagoonal environment, based on the presence of the monospecific gastropods (predominantly *Turritellidae*; see Öztürk et al., 2003) that are in life position. A similar setting has been inferred for the Holocene Sabkha Boujmel Formation in coastal southeast Tunisia (Lakhdar et al., 2006). In general, the cements of the various grainstone facies are characterised by sparite rim cements that probably represent a vadose diagenetic environment. In numerous studies, sparite rim cements are interpreted to represent a subaerial vadose diagenetic environment (e.g., McLaren, 1993; Frébourg et al., 2008; Mauz et al., 2015). The $\delta^{18}O$ and the $\delta^{13}C$ data plot within, or near, the meteoric cement field (Fig. 9a), which suggests that the cements formed within a vadose rather than a phreatic diagenetic environment. Fig. 9b compares the Kyrenia Range stable isotope data with Pleistocene aeolianites in Bermuda (Gross, 1964). The Kyrenia Range terrace data have $\delta^{13}C$ ratios within the range of the Bermuda aeolianites; however, $\delta^{18}O$ ratios are slightly lower, suggesting subtly different subsurface water conditions probably related to the basement geology of the Kyrenia Range, which influenced the composition of cement-precipitating pore fluids (Nelson and Smith, 1996).

The D1 facies breccia is interpreted as a proximal, near-coastal-marine deposit, based on the presence of large, angular clasts of lithic material, *in situ* coral and by virtue of being interbedded with deltaic facies (F7 gravel facies) (Fig. 6, log 25). The D2 facies conglomerate records short-lived, high-energy, near-coastal flows (e.g., storm events), as suggested by the presence of the poorly sorted, angular clasts of lithic material (Fig. 6, log 26). Bioclasts, grainstone clasts and basement lithologies are all likely to have been locally reworked in a nearshore setting.
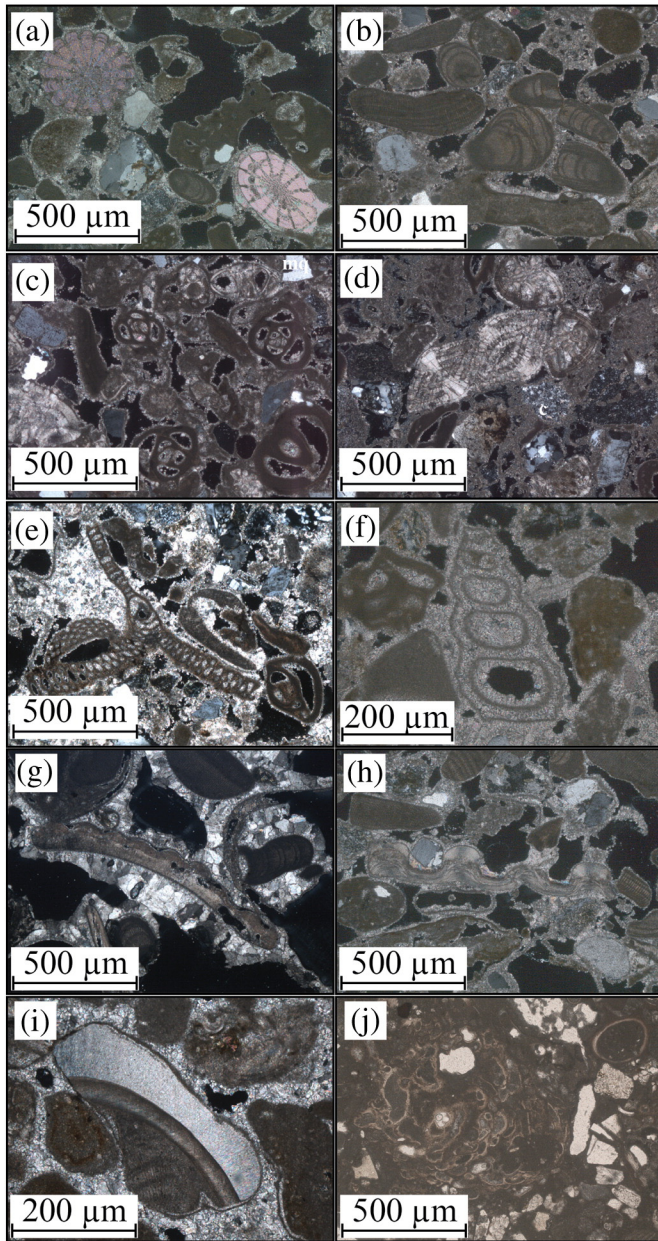
Fig. 7. Photomicrographs of carbonate grainstones on the northern flank of the range. (a) echinoderm plates; (b) reworked, well-rounded calcareous red algae; (c) *Miliolida* (benthic foraminifera); (d) *Neorotalia* (benthic foraminifera); (e) *Peneroplidae* (benthic foraminifera); (f) *Textulariidae* (benthic foraminifera); (g) *Pecten* (bivalve fragment); (h) Oyster (bivalve fragment); (i) reworked serpulid worm tube; (j) calcareous green algae.

Fig. 8. Photomicrographs of clastic grains in grainstones on the northern flank of the Kyrenia Range. (a) monocrystalline quartz; (b) polycrystalline quartz; (c) plagioclase; (d) chert; (e) diabase; (f) metacarbonate rock; (g) carbonate grainstone; (h) foraminifera-rich marl.

grainstone, and bored clasts (see Clifton et al., 1973; Bourgeois and Leithold, 1984), as reported from the Pleistocene terrace deposits of the Spanish Mediterranean and Atlantic coasts (Zazo et al., 2003).

6.8. Facies association E: carbonate aeolian deposits

The E1 and E2 aeolian grainstones facies characterise all of the terraces on the northern flank of the range (Table 6). These facies are fine to medium grained, the grains being well sorted and well rounded. Calcified root casts are commonly preserved throughout the E2 facies but only near the uppermost surface of the E1 facies. The roots are generally replaced by calcite with no organic material remaining. The main differences between the E1 and the E2 facies relate to the type and size of sedimentary structures present. The E1 facies grainstone comprises 1 to 2 m-thick depositional units, which are characterised by planar cross-bedding, in which foresets dip at >30° (Fig. 4, log 1; Fig. 5, log 12; Fig. 6, log 22). In contrast, the E2 facies comprises 1 to 3 m-thick trough cross-bedded units, with foresets dipping at 20°–40°. In addition, the E2 grainstone facies forms thicker aeolian deposits within the K5 terrace compared to to the E1 facies grainstone deposits in older terrace systems. Both the E1 and E2 facies aeolian grainstones are well lithified, with sparite cement coating grains and partially infilling pores. Well-preserved remains of the pygmy hippopotamus *Phanourios minutus* are occasionally observed within the E1 facies grainstone (Baroz,

The D3 facies conglomerate represents a shallow-marine environment, which was affected by occasional high-energy events (e.g., storms), as suggested by the repeated beds of conglomerate with well-rounded clasts and the well-developed normal grading (Fig. 6, log 15). The presence of clasts including lithic and bioclastic material, such as bivalves, gastropods, coral, and serpulid worm tubes suggests the reworking of fluvial and marine deposits. Interbedded with the D3 conglomerate facies, the poorly lithified mudstone with well-preserved biogenic material (Fig. 6, log 15) is indicative of low-energy deposition between high-energy events. The D4 facies conglomerate represents a pebble beach environment, as suggested by the well-rounded clasts, coast-parallel palaeocurrents (toward the west), interbedded aeolian
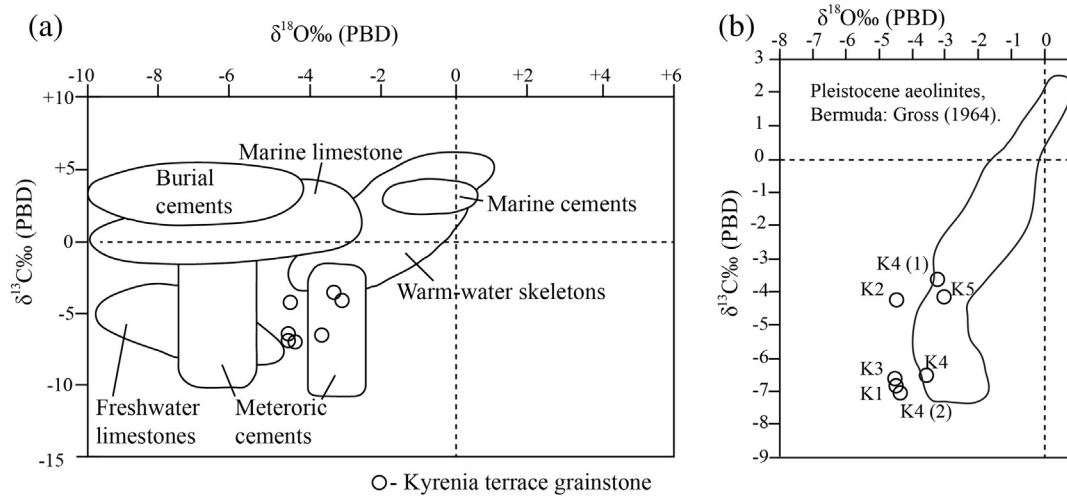
Fig. 9. δ¹⁸O and δ¹³C plots of carbonate cement from Pleistocene marine and aeolian grainstones from northern Cyprus; (a) adapted from Hudson (1977) and from Nelson and Smith (1996); (b) Pleistocene aeolianite field, adapted from data in Gross (1964).

1979). The E2 facies grainstones are commonly incised to form wave-cut platforms and tidal notches along the coast.

6.9. Interpretation: aeolian carbonate deposition

The E1 and E2 facies grainstones accumulated as coastal aeolian dunes, as indicated by the presence of high-angle (>30°) foresets (1–3 m thick), root traces, vertebrate bones, well-rounded and well-sorted clasts, and also mixed bioclastic and clastic material (as defined by Frébourg et al., 2008). The E1 aeolian grainstone facies is interpreted as an inland component of the dune system, which is preserved within the K2 to K4 terrace systems. In contrast, the E2 aeolian dune deposits are seen as coastal dunes, as observed in situ within the K5 terrace system. The abundance of palaeoroots throughout the E2 facies suggests multiple periods of low sedimentation during which vegetation developed. By contrast, the restriction of palaeoroots to the uppermost parts of the E1 facies suggests a single phases of deposition, followed by vegetation development. The total replacement of roots (even in the youngest terrace) with carbonate and the presence of vadose cement within the grainstones suggest meteoric-water lithification. Worldwide occurrence of similar Pleistocene near-coastal carbonate aeolian dune deposits (Brooke, 2001) include examples from Mallorca (Fornós et al., 2009), the Bahamas (Kindler and Mazzolini, 2001), western Australia (Hearty and O'Leary, 2008), and southern Cyprus (Poole and Robertson, 2000). The bioclastic material originated within a sub-aqueous coastal setting, followed by subaerial exposure, erosion, and wind reworking to form aeolian dunes. Planar (E1 facies) and trough-shaped (E2 facies) cross bedding within the dunes represent straight and sinuous dunes, respectively.

6.10. Facies association F: fluvial deposits

Fluvial deposits are represented by interbedded sequences of mudstone and conglomerate together with palaeosols (Table 7; Fig. 4–7). The facies within each terrace system varies considerably in geometry, thickness and sedimentary structures.

The mudstone facies (Facies F1; Table 7) is widely distributed within all of the terrace systems. Mudstone is typically fine to medium grained, partially lithified and generally massive, with no preserved sedimentary structures. Mudstone beds vary in thickness from 50 cm to 4 m. Conglomerate facies include: <40 cm thick clast-supported lenses (F2 facies), >1 m thick clast-supported lenses (F3 facies), bedded

conglomerate (F4 facies), colluvial conglomerate (F5 facies), and cross-bedded gravel (F6 facies) (Table 7). The F2 and F3 facies conglomerate are interbedded with the F1 facies mudstone. Lenses of F2 facies conglomerate are <40 cm thick individually and vary in length from 1 to 10 m (e.g., Fig. 4, log 2; Fig. 5, log 13; Fig. 6, log 28). The clasts within the F2 lenses are subangular and moderately to well sorted, with poorly developed normal grading and imbrication. In contrast, the F3 facies conglomerate is made up of 10 to 30 cm-thick lenses, typically 2–4 m across (Fig. 4, log 3; Fig. 5, log 13; Fig. 6, log 25). The clasts again show poorly developed normal grading. Although subangular, the clasts are better sorted than those within the F3 facies conglomerate. The combined thickness of the interbedded F2 and F3 facies conglomerate and the F1 facies mudstones ranges from 1 to 10 m, as exposed near the village of Bahçeli (Kalograi) on the northern coast (Fig. 6, log 28). The F4 facies conglomerate (Table 7) is exposed at several localities on the northern and southern flanks of the range (e.g., Arapköy (Klepini) and Nergisli (Genagra) villages) (Fig. 1). Where observed, the deposit is 1–5 m thick and is made up of parallel beds, 10–30 cm thick, which are normally graded with well-sorted subangular to subrounded clasts (1–20 cm in size). The F5 facies conglomerate is massive and poorly sorted, in beds 1–3 m thick and contains subangular clasts (1–40 cm in size). This facies is interbedded with the F1 facies mudstone and with the F2 to F4 facies conglomerate.

Dark maroon to dark red-coloured palaeosols, defined as facies F6 (Table 7), are preserved within all of the fluvial terrace systems (Figs. 4–6). The palaeosols form 30 to 50 cm-thick beds that are laterally continuous for up to 10 m. In places, the palaeosols are overlain by or cut by conglomerate lenses. The palaeosols commonly contain moderately to well-developed caliche, locally known as havara (Schirmer, 1998). In general, the palaeosols are mainly interbedded with mudstone or include small conglomerate lenses (<10 cm thick and <2 m long).

The F1–F3 mudstones and conglomerate lenses within the K2 and K4 terrace systems commonly contain three to four light- to dark-brown palaeosols, interbedded at the base of the sequence with predominantly F1 facies mudstone (Fig. 4, logs 2 and 5). In contrast, dark brown palaeosols are commonly interbedded throughout the F1–F3 facies mudstones and conglomerates of the K3 terrace (Fig. 5, logs 8 and 9). In addition, dark brown palaeosols are interbedded with the E1 aeolian grainstone facies within the K1 and K4 terrace systems (Fig. 6, logs 20 and 31).

One gravel facies (F7 facies; Table 7) is only known from the lowest terrace (K4) on the northern flank of the range (Fig. 6, log 25). This is

characterised by low-angle (<30°) foresets, each 30–50 cm thick. Clasts are subrounded to well-rounded and 1–5 cm in size, although outsized clasts (10–30 cm diameter) are also locally present.

The clasts within the F7 conglomerate facies are predominantly re-crystallized limestone and dolomite derived from the Mesozoic Trypa (Tripa) Group. Chalk, basalt and redeposited limestone (calcarenite and breccia) clasts came from the late Cretaceous-Paleogene Lapithos (Lapta) Group. In addition, clasts of mudstone and sandstone were de-rived from from the upper levels of the Lapithos (Lapta) Group and/or from the overlying late Eocene to late Miocene Kythrea (Diğermenlik) Group. The greatest variation in clast lithology occurs in relatively distal deposits (>5 km from source) on the southern flank of the range.

6.11. Interpretation: fluvial processes

The lenticular F2 and F3 facies conglomerates are interpreted as repeatedly incised erosional channels that were mostly infilled by high-energy debris-flow deposits. The thickest of the facies (F3) rep-resents multiple debris-flow events. The F4 facies conglomerate is characterised by tabular, laterally continuous conglomerate beds, free of mudstone (F1 facies) and is therefore interpreted as having taken place over an extended time period, probably from perennial streams; unlike the F2 and F3 facies, they represent short-lived 'flashy' events. In addition, the F5 facies conglomerate is associated with the F2 to F4 facies conglomerates in all of the terrace systems. The F5 facies conglomerate is interpreted as the product of slope wasting (colluvium). Similar interbedded F1- to F5-type facies are known from Pleistocene fluvial systems, as in the Himalayas (Thomas et al., 2002; Kumar et al., 2003), western Turkey (Maddy et al., 2008), southern Italy (Westaway and Bridgland, 2007), and southern Cyprus (Poole and Robertson, 1998; Waters et al., 2010).

The palaeosols occur within the fluvial deposits of the K2 to K5 ter-race systems on both the northern and southern flanks of the range. In many cases, two to four stacked palaeosol occur in a single outcrop (Figs. 4–6). The stacked palaeosols within each of the fluvial deposits are interpreted as short-lived periods of relatively low fluvial sediment accumulation versus high rates of pedogenesis (Kraus, 1999). The palaeosols are, for example, similar to palaeosols described from eastern central Italy (Celma et al., 2015) and from along the Israel coast (Frechen et al., 2004). Such palaeosols are interpreted as representing warm, humid climatic conditions during late Pleistocene interglacial phases. The well-developed calcrete (havara) within the palaeosol hori-zons is interpreted as having formed under semi-arid conditions (Arakel, 1982; Candy and Black, 2009).

The localised F7 facies gravel is interpreted as a small example of a Gilbert-type delta, based on the well-rounded clasts, low-angle gravel foresets (50 cm thick), and the well-sorted nature of the clasts. Similar Gilbert-type deltaic environments occur in the Gulf of Corinth (Rohais et al., 2007) and in the Calabrian Arc, southern Italy (Fabbricatore et al., 2014).

7. Facies relations and correlations

The specific facies exposed in each terrace system combine to pro-duce distinctive depositional systems, ranging from intramontane la-custrine, massive slope wasting, shallow-marine, fluvial, and aeolian depositional environments. We primarily focus on the northern flank of the range because the marine facies there allow detailed correlation and interpretation.

The non-marine K0 and K1 terrace deposits can be correlated along both the northern and southern flanks of the range, based on height above mean sea level and facies type. The megabreccias, debris-flow deposits and colluvial facies are all located above 300 m AMSL, within ca. 500 m laterally of the axis of the range.

The K2 to K5 terrace systems include a range of marine to non-marine facies, which can be correlated within each of the terrace

systems (Figs. 4–6 and 10). The K2 terrace forms a major topographic feature along the northern flank of the range, reflecting its height compared to the K3 terrace (Fig. 10a). The C1 facies grainstones are preserved from 140 to 170 m AMSL on the northern flank and can be correlated with equivalent deposits at Lapta (Lapithos), Arapköy (Klepini), and Kaplıca (Davlos) villages representing the earliest part of the K2 terrace (Fig. 4, logs 1–6). The basal marine facies is overlain by aeolian grainstones at Lapta (Lapithos) village, (E1 facies) (Fig. 4, log 1) and by fluvial deposits at Arapköy (Klepini) village (F1–F3, F6 fa-cies) (Fig. 4, logs 2–6). Different fluvial deposits at equivalent heights are likely to represent various parts of broadly contemporaneous fluvial drainage systems.

The K3 terrace system varies in height above mean sea level but is in-variably significantly lower than the K2 terrace system (Fig. 5). The to-pographically lowest deposits are preserved near Çatalköy (Agios Epikitos) village at ca. 50 m AMSL (Fig. 5, logs 7 and 8), comprising a basal-marine deposit and fluvial deposits. Further inland, the K3 terrace deposits are preserved at a significantly higher level (ca. 140 m AMSL), between Arapköy (Klepini) and Beşparmak (Trapeza) villages (Fig. 5, logs 9–11). The terraces form geomorphic surfaces that dip gently away from the range toward the coast (Fig. 10a).

The K4 terrace system is observed near the northern coast and up to ca. 1.5 km inland. Several different shallow-marine environments characterise the base of the K4 terrace system along the northern flank of the range. The K4 terrace basal littoral-marine environment can be recognised and correlated along the northern coast (Fig. 6, logs 14, 15, 19, 21, 22). The C2 and C3 facies grainstone along the northern coast (Fig. 6, logs 16, 17, 21, 22, 29) represent a wave-dominated shallow-marine environment, in which biogenic material was intro-duced from littoral-marine environments. Interbedded with the upper part of the littoral-marine environment are conglomerate-filled chan-nels (Fig. 6, logs 23, 27) (Fig. 10b), deltaic gravels (Fig. 6, log 25) (Fig. 10c) and lagoonal deposits (Fig. 6, logs 26 and 29). The conglomer-ate channels that are interbedded with the marine deposits are com-monly exposed near (<100 m) inland fluvial drainage systems. The fluvial drainage systems are, therefore, interpreted as a source of mate-rial for submarine channels. The interbedded conglomerate lenses and marine grainstone deposits are interpreted as high-energy gravity flows into a littoral-marine environment. In contrast, the interbedded deltaic and shallow-marine deposits are interpreted as transgressive events, as indicated by the lateral continuity of the marine deposits (Fig. 6, log 25). The equivalent heights above mean sea level of the beach deposits suggest that they were contemporaneous with the littoral-marine deposits (Fig. 6, log 20) (Fig. 10d).

The non-marine aeolianite and fluvial deposits of the K4 terrace are preserved further inland, and at topographically higher levels relative to the marine deposits of the terrace (e.g., Fig. 6, logs 20–25). The aeolian deposits are preserved above marine deposits near the coast, for exam-ple, at Sadrazamköy (Livera) village (Fig. 10e), Alagadi beach and Küçükerenköy village (Fig. 6, logs 14, 21, 22, 29), and also overlie fluvial deposits farther inland (e.g., at Mersinlik) village (Fig. 6, log 31) (Fig. 10f). The non-marine aeolian deposits extend continuously inland, commonly for ca. 1.5 km. Aeolian deposits of the K4 terrace system con-tinue between the K4 and K3 terrace surfaces, making identification of terrace boundaries difficult. The fluvial deposits form a series of drain-age catchments within the K4 terrace system (Fig. 6, logs 20, 28, 31), which can be correlated with the drainage catchments of older terraces, such as at Arapköy (Klepini) and Esentepe (Agio Amvrosios) villages (Figs. 4 and 6). In places, the fluvial deposits are conformably overlain by aeolianites (Fig. 6, log 31; Fig. 10f).

The K5 terrace system near the coast is predominantly made up of aeolian grainstone (E2 facies) (Fig. 10g, h). Correlation of these terrace deposits was achieved based on the predominant facies being E2 facies aeolianites that are all exposed near sea level along the northern coast. This terrace is topographically lower than the K4 terrace in most places; however, in several areas the K5 terrace aeolianite overlies the K4
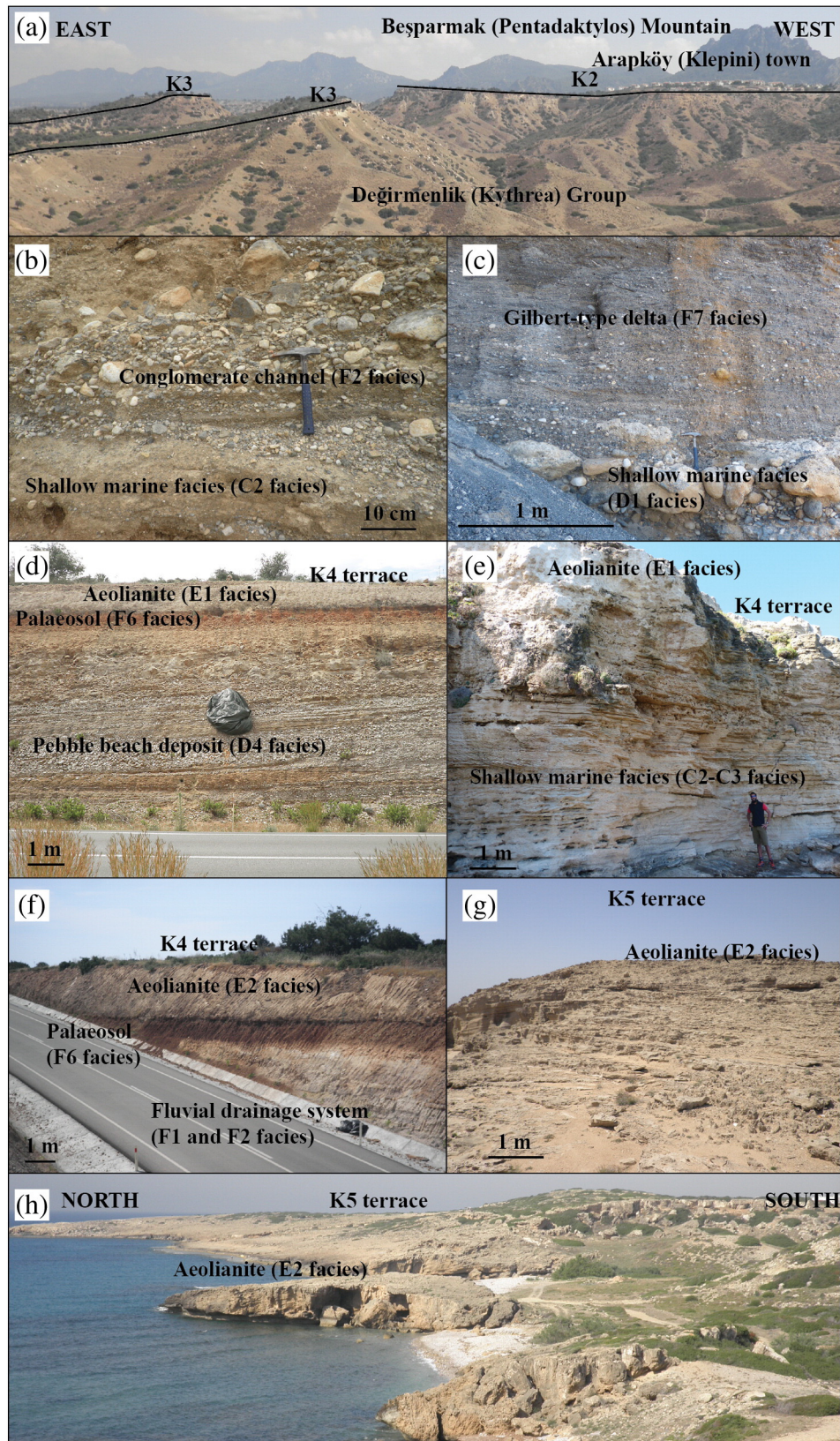
Fig. 10. Photographs showing key features of the terrace deposits in the Kyrenia Range, (a) overview photograph of the K2 and K3 terrace systems at Arapköy (Klepini) village; (b) conglomerate lenses interbedded with marine grainstone; (c) marine grainstone breccia interbedded with cross-bedded deltaic gravel; (d) pebbly beach deposits overlain by aeolian grainstone; (e) marine grainstone overlain by aeolian grainstone; (f) fluvial deposits with palaeosols overlain by aeolian grainstones; (g) massive trough cross-bedding in aeolian grainstone; (h) aeolian grainstone along the northern coast of the range.
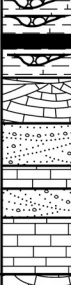
Composite logs from northern flank terraces of the Kyrenia Range

Terr.	Log	Description	Terr.	Log	Description
K0		Megabreccia, high-energy debris-flow sheets and lacustrine deposits	K3		Terrace locally downcut into the K2 terrace. Basal marine deposit overlain by non-marine deposits, including aeolianites, interbedded channelised debris-flow deposits and mudstones.
K1		Colluvium, locally overlain by aeolianites and palaeosols.	K4		Basal marine deposit overlain by non-marine deposits including aeolianites, interbedded channelised debris-flow deposits and mudstones. A marine deposit is interbedded part way through the deltaic deposit.
K2		Marine deposits overlain by non-marine deposits, including aeolianites, interbedded channelised debris-flow deposits and mudstones.	K5		Aeolianite preserved above marine transgression in the lower part of the deposit. Fluvial systems eroded older terraces made up of unconsolidated conglomerates.

Fig. 11. Composite sedimentary log, summarising the various facies of the K0 to K5 terrace systems on the northern flank of the Kyrenia Range.

terrace marine deposit directly, for example, at Tatlısu (Akanthou) village (Fig. 6).

In summary, the uppermost K0 terrace system represents the interbedding of lacustrine and megabreccia facies within the central and highest parts of the Kyrenia Range (Fig. 11). The K1 terrace system represents colluvial and aeolian deposits, and also palaeosol formation along the northern and southern flanks of the range (Fig. 11). The K2 to K5 terrace systems represent marine transgressions to form littoral-marine environments, followed by marine regressions associated with channelised debris-flow deposits and aeolian dunes (Fig. 11). As an exception, the K4 terrace system exhibits an additional thin, marine transgressive event (Fig. 11).

8. Sedimentary development through time

8.1. Lacustrine facies (K0 terrace)

The oldest K0 terrace deposits within the central Kyrenia Range represent small lacustrine basins, which formed in topographic lows within a relatively rugged relief. Other potential lacustrine deposits in the central range and farther east were inaccessible during this study.

One prominent lacustrine basin, south of Beşparmak (Pentadaktylos) Mountain, was orientated ca. E–W, approximately parallel to the axis of the range. The topographic low, which became a lake, is located in the vicinity of a thrust contact between erosionally resistant metacarbonate rocks of the Trypa (Tripa) Group to the north and much more easily eroded pelagic chalks, marls, sandstones, and basic volcanics of the Lapithos (Lapta) Group to the south. A zone of lithological weakness and rheological contrast was exploited by fluvial erosion to create a

channel. This was followed by damming, possibly by landsliding, to create a lake. However, any such damming material is no longer preserved. The interbedded relationship of the lacustrine sediments and the lowest megabreccia deposits indicates that steep and unstable slopes fringed the lake.

The lacustrine deposits are inferred to have accumulated during early stage uplift of the Kyrenia Range. The youngest shallow-marine and non-marine sediments that accumulated prior to major surface uplift of the Kyrenia Range are exposed within the Mesaoria (Mesorya) Basin to the south and are inferred to be of late Pliocene to early Pleistocene age (Baroz, 1979; Hakyemez et al., 2000; Harrison et al., 2008; Palamakumbura et al., 2016b). The A1 to A3, lacustrine deposits are likely to be of early to mid-Pleistocene age.

8.2. K0 and K1 megabreccia facies

The B1 facies megabreccias are only preserved near cliffs of Mesozoic metacarbonate rock, near the highest levels of the central range. The megabreccias are interpreted as representing a relatively short-lived phase of erosion and extensive mass wasting of Mesozoic metacarbonate rocks (Trypa (Tripa) Group). Based on field observations, three key factors appear to have controlled megabreccia formation: (1) selective erosion of source lithologies, (2) pre-existing major fractures and faults, and (3) rapid uplift.

Firstly, the well-lithified, typically thick-bedded to massive Mesozoic metacarbonate rocks are relatively resistant to erosion and have the potential to support steep slopes (Fig. 12a). For this reason alone, megabreccias tended to form related to erosion of these rocks. Similar megabreccias do not occur in other areas (e.g., eastern Kyrenia Range)
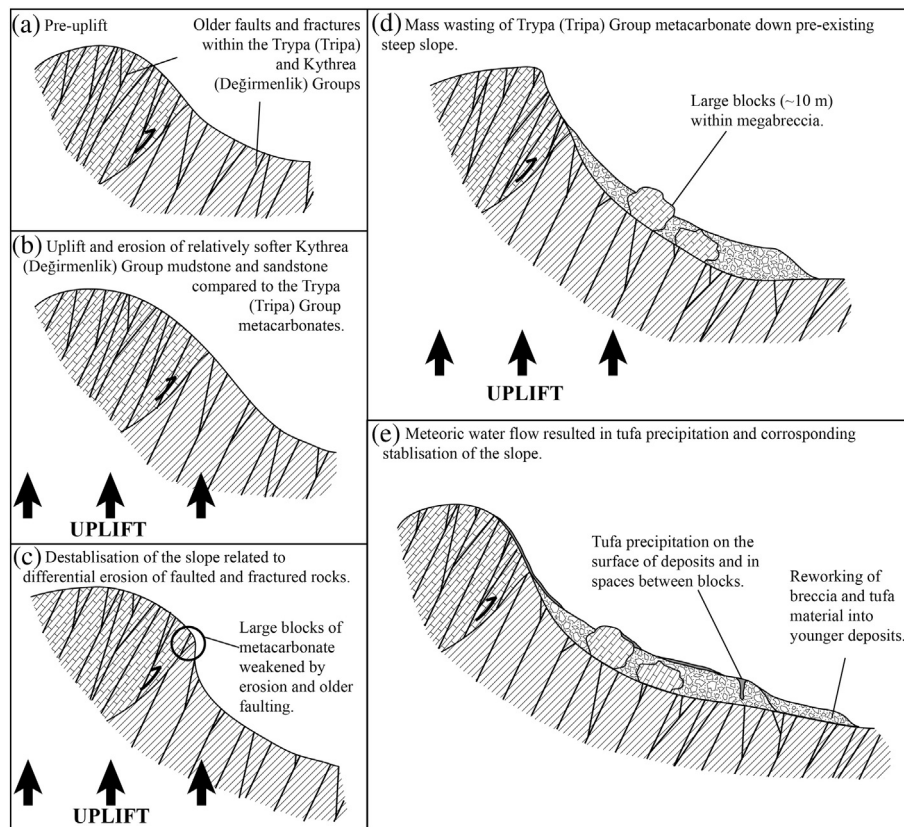
Fig. 12. Schematic diagram showing the inferred process of fault-scarp degradation that controlled the formation of the K0 terrace system megabreccia facies.

where the basement lithologies were more easily eroded (e.g., chalks and marls of the Lapithos (Lapta) Group).

Secondly, the metacarbonate rocks (and other lithologies, where exposed) are dissected by an array of mostly high-angle faults (Fig. 12a), many of which are orientated generally N-S based on kinematic measurements (i.e., fault plane orientation; trend and plunge of fault striations) (Robertson and Kinnaird, 2016). The faulting developed in several stages, principally during the early to mid Eocene and the late Miocene-earliest Pliocene (Ducloz, 1972; Baroz, 1979; Robertson and Kinnaird, 2016). Faults and fractures are typically spaced tens of centimetres apart, whereas through-going faults are spaced several metres to several tens of metres apart. As a result, erosion of highly fragmented metacarbonate rocks typically produced clasts and blocks with dimensions ranging from tens of centimetres to several tens of metres in size.

Thirdly, we infer that the mass wasting was greatly accentuated by rapid tectonically driven uplift of the Kyrenia Range (Fig. 12c, d). Oversteepened slopes repeatedly collapsed to form megabreccia, resulting in progressive slope degradation. The slopes were sufficiently steep and unstable to generate the exceptionally coarse clastic talus. Without contemporaneous uplift, lithological hardness differences and pre-existing faults and fractures by themselves would have resulted in less accentuated slope erosion, and deposition of fining-upward sequences as slopes gradually eroded and matured.

Comparable breccia formation can be triggered by movement on subaerially exposed, active faults (e.g., Leeder et al., 1991; Cavinato et al., 2002). For example, fault talus commonly accumulates on the footwalls of high-angle extensional faults (e.g., Stewart and Hancock, 1990; Basilone, 2009; Sanders et al., 2009). However, the field relations in the Kyrenia Range do not support an origin of the megabreccias related to mass wasting of active (coseismic) fault scarps. Where the talus fans can be traced back to the source metacarbonate cliffs, there is no evidence that these surfaces were active faults. Indeed, as noted above, most of the observed faults are orientated ca. N-S, approximately

at right angles to the strike of the megabreccia deposits. Some faults are known to have been active within the Kyrenia Range during the Pleistocene (McCay and Robertson, 2012b; Robertson and Kinnaird, 2016). However, these are rare, generally orientated at a high angle to the range, and occur independently of the ca. E-W trending megabreccias.

After the main phase of megabreccia development had ended, the B1 facies formed in response to locally variable downslope reworking of colluvium (Fig. 12e). Similar slope processes affected other areas, for example, parts of the eastern range that were dominated by the less competent pelagic carbonates and volcanics of the Lapithos (Lapta) Group (e.g., near Tirmen (Trypimeni) village) (Fig. 1). The altitude above sea level of these areas was lower, and the slopes less steep than in the central range such that the resulting erosional talus was correspondingly less abundant and also finer grained.

The final stages of the K0 terrace development in all areas included karstic weathering and tufa precipitation, both onto the surface and within the megabreccias (Fig. 12e). Reworked karstic material is found within the B3 colluvium facies showing that karstic weathering was active by the time the megabreccias had begun to form and, indeed, has been ongoing (either episodically or continuously) until recent time.

8.3. Marine and non-marine terrace systems

The K2 to K5 terrace systems represent marine to non-marine environments on the northern flank of the range and also exclusively non-marine environments on the southern flank of the range. The basal facies of all of the K2 to K5 terraces on the northern flank are mostly marine. In each case, a marine transgression created a littoral-marine environment (Fig. 13), although not all of the components of this setting are preserved within all of the terraces. Each terrace system includes fluvial deposits, which are interbedded with, and overlie, basal marine deposits (Fig. 13). Aeolian dune deposits cover both the marine and the fluvial deposits, predominantly near the palaeo-coast (Fig. 13).
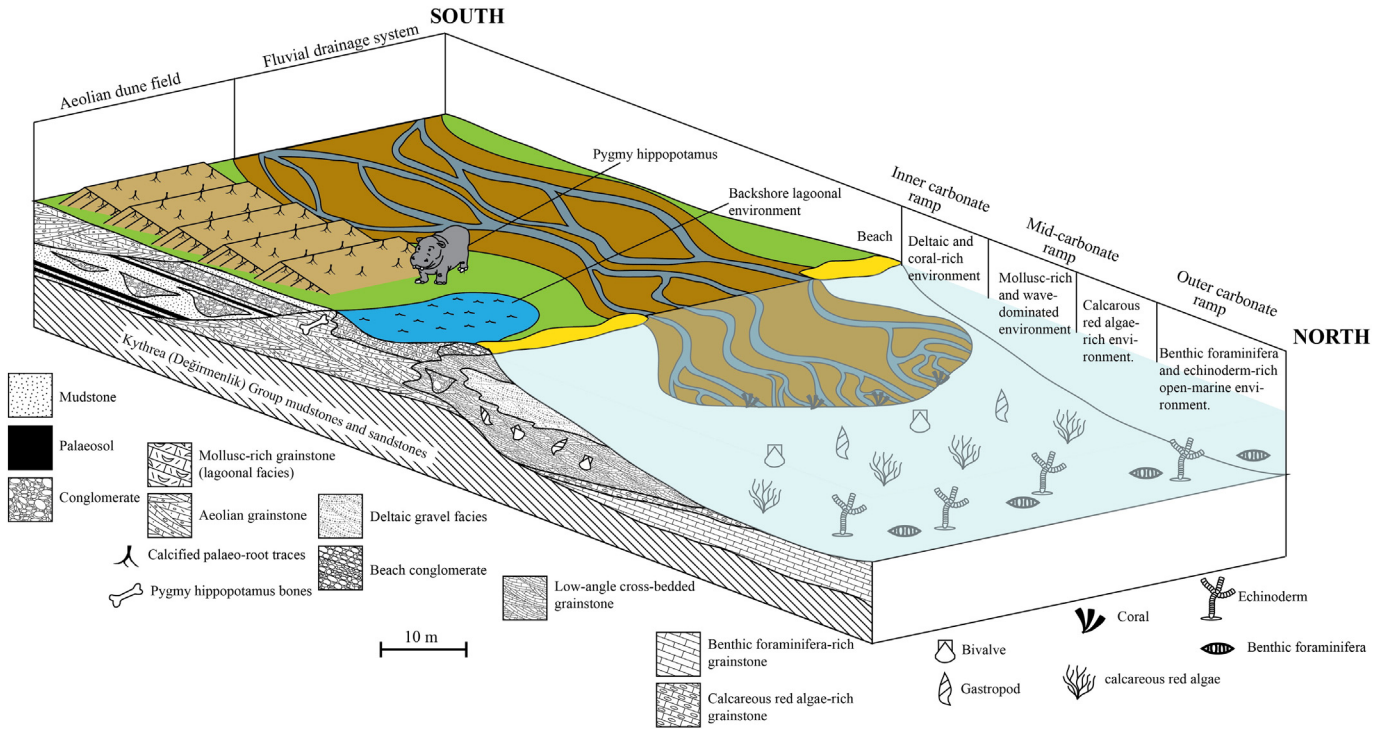
Fig. 13. Block diagram illustrating the various depositional environments and sedimentary relationships for each of the K2 to K5 terrace systems on the northern flank of the Kyrenia Range.

Each entire marine, fluvial, and aeolian terrace depositional system was later uplifted and subaerially dissected to varying degrees. While older terrace deposits were being uplifted, the subsequent terrace was already beginning to form at a lower topographic level, with its own marine, fluvial, and aeolian accumulation. Similar cyclic sequences were repeated to form the K2 to K5 depositional systems, culminating in the present staircase terrace topography (Fig. 14).

On the southern flank of the range, the K2 to K5 terraces are represented by fluvial drainage systems. These are generally similar throughout all of the terrace systems, comprising interbedded F1 to F6 facies. Each
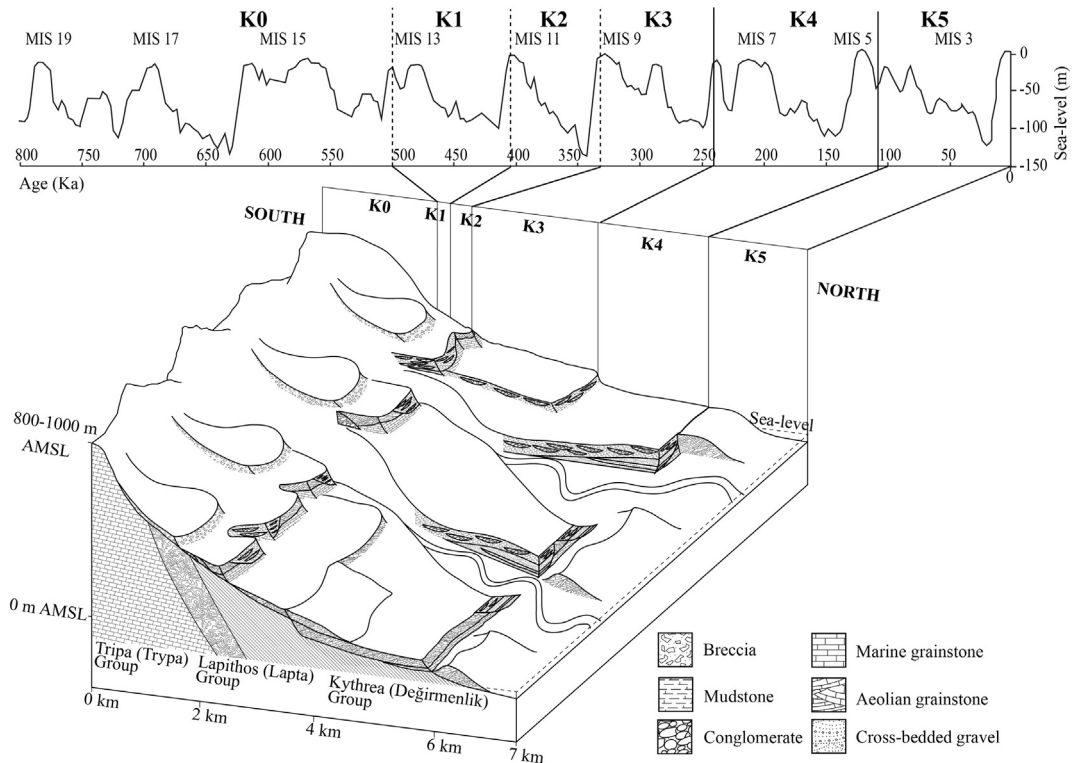
Fig. 14. Block diagram showing an interpretation of the depositional environments of the K0 to K5 terraces, correlated with the global eustatic sea-level curve (sea-level curve from Siddall et al., 2006).

terrace system represents a series of subparallel fluvial catchments, draining southwards away from the range into the intermontane Mesaoria (Mesarya) Basin. The fluvial drainage of each terrace system typically eroded and reworked one, or several, older fluvial terrace deposits.

9. Age constraints on terrace development

A good understanding of the terrace depositional system through time requires absolute age constraints, as summarised below. Uranium series (U-series) and optically stimulated luminescence (OSL) dating have been carried out on deposits from the K4 and K5 terrace systems on the northern flank of the Kyrenia Range (Palamakumbura et al., 2016b). The U-series dating utilised solitary corals from the D1 and D3 facies marine conglomerate (Table 5) that are approximately *in situ*, yielding ages of 127 and 131 ka from the D1 facies and 243 ka from the D3 facies. The D1 facies marine conglomerate is interbedded with the coastal deltaic deposit (F7 facies gravel) that is interpreted as representing a short-lived marine transgression. The D3 facies marine conglomerate is located at the base of the K4 terrace system and is overlain by aeolian grainstones (E1 facies), which are interpreted to represent a marine transgression followed by a gradual marine regression. The dated marine deposits of the K4 terrace can be correlated with marine isotope stages (MIS) 5 (ca. 130 ka) and 7 (ca. 243 ka), which are interpreted to reflect global sea-level maxima (Siddall et al., 2006).

OSL dating was carried out on the basal aeolian grainstone (E2 facies) of the K5 terrace system from the northern coast, producing ages of 76 and 53 ka (Palamakumbura et al., 2016b). The OSL ages from the K5 terrace aeolian grainstone can be correlated with MIS 4, a glacial period that represents a global sea-level minimum. The OSL ages, therefore, suggest that major aeolian deposition took place during global glacial periods. Aeolian deposition related to an arid climate during Pleistocene glacial stages is also documented from several other areas, including the northern Appenines, Italy (Ghinassi et al., 2004), and northwestern Europe (Kasse, 2002). In addition, coastal aeolian deposits in the western part of the Kyrenia Range have recently been dated as MIS 4 using OSL (Erginal et al., 2012). The relative ages of the younger (i.e., lower) marine terraces can also be inferred from their associated fauna (e.g., gastropod *Strombus bubonius*) (Galili et al., 2015).

10. Discussion

The new facies evidence presented here suggests that the dominant control of deposition was the surface uplift of the Kyrenia Range during the Pleistocene. In addition, Pleistocene eustatic sea-level change, climatic change and autocyclic processes were also important controls on deposition.

10.1. Tectonic uplift

The uplift of the Kyrenia Range from near sea level in the late Pliocene to a height of up to 1024 m during the Pleistocene is generally accepted as being tectonically driven (Robertson and Woodcock, 1986; Kempler and Ben-Avraham, 1987; Harrison et al., 2008; Calon et al., 2005; McCay and Robertson, 2012b; Robertson and Kinnaird, 2016). The driving mechanism is believed to relate to continental-scale collisional processes (Barka and Reilinger, 1997; Fernandes, 2003; McClusky et al., 2003; Robertson et al., 2012). The Kyrenia Range was drastically uplifted in response to the reactivation of a deep-seated tectonic lineament, which developed during pre-existing phases of late Cretaceous, early–mid Eocene, and latest Miocene-earliest Pliocene deformation. The overall tectonism included burial metamorphism, thrusting, folding, and strike-slip/transpression (Anastasakis and Kelling, 1991; Harrison et al., 2012; Robertson et al., 2012, 2014, McCay and Robertson, 2012b; Welford et al., 2015; Robertson and Kinnaird, 2016). The previously fragmented, rising lineament

underwent rapid differential erosion to form the K0 megabreccias, influenced by the very hard Mesozoic metacarbonate rocks and the poorly consolidated Neogene mudrocks and sandstones, where present.

The megabreccias of the K0 terrace were dominantly controlled by a major pulse of tectonically driven surface uplift. The stepped lower-level terraces (K1 to K5) formed sequentially during ongoing but less dramatic uplift. The quantitative dating studies suggest that the Kyrenia Range was uplifted at 1.2 to 2 mm/year during the early Pleistocene, slowing to 1.0 to 0.7 mm/year during the middle Pleistocene, and finally to <0.2 mm/year during the late Pleistocene (Palamakumbura et al., 2016b). These rates are comparable to the inferred uplift rates of the Troodos Massif in the south of Cyprus, whereas adjacent tectonically active areas (e.g., southern Anatolia; Levant coast) experienced significantly slower Pleistocene uplift rates (see Palamakumbura et al., 2016b).

10.2. Eustatic sea-level change

Glacio-eustasy is well known to have influenced Pleistocene and earlier shallow-marine and non-marine deposits (e.g., Blum and Törnqvist, 2000; Hall and Nichols, 2002; Zazo et al., 2003; Ferranti et al., 2006; Quigley et al., 2007; Elmejdoub and Jedoui, 2009). Some recent studies of Pleistocene uplifted deposits have used geomorphological methods (e.g., digital elevation models) to map and correlate terraces that were influenced by glacial and interglacial cycles (e.g., Bridgland and Westaway, 2008; Pedoja et al., 2014). Several studies have focused on the late Pleistocene development of terraces in the Mediterranean, including fluvial depositional and erosional processes (Macklin et al., 2002; Maddy et al., 2008; Kober et al., 2013; Andreucci et al., 2014; Main et al., 2016). Other studies investigated coastal-marine terraces of late Pleistocene age with a view to understanding the interaction of tectonic uplift versus subsidence and influence of glacially controlled cyclicity (Reyss et al., 1998; Zazo et al., 2003; Zecchin et al., 2004; Ferranti et al., 2006; Dodonov et al., 2008).

Eustatic sea-level change controlled the transgressive-regressive cycles, as documented in each of the terrace systems along the northern margin of the Kyrenia Range. Oscillations in eustatic sea level during the Pleistocene, as inferred in many areas (e.g., Zachos et al., 2001; Siddall et al., 2006), exerted a major influence on the K2 to K5 terrace deposits, specifically (Fig. 14). The interbedded relationships of the marine and fluvial facies of the K4 terrace indicate contemporaneous deposition (Fig. 6, logs 23, 25, 27; Fig. 10b, c). The U-series dating of the marine deposits of the K4 terrace indicate marine deposition during an interglacial (Palamakumbura et al., 2016b). The facies relationships and U-series dating also suggest that the marine and fluvial deposition within the K4 terrace occurred during interglacial stages. OSL dating of aeolianites within the K5 terrace indicate multiple phases of aeolian deposition during a glacial period (Palamakumbura et al., 2016b). The aeolianites of the K4 and K5 terrace are observed to stratigraphically overlie marine and fluvial facies (Fig. 6, logs 29 and 31; Fig. 10e, f). The aeolianites of each terrace mostly accumulated in near-coastal areas, often conformably above marine deposits. Large volumes of carbonate material were reworked from contemporaneous, shallow-marine bioclastic carbonate, and/or pre-existing aeolianites (Brooke, 2001; Frébourg et al., 2008). Each terrace sequence is, therefore, interpreted to represent an initial phase of marine and fluvial deposition during an interglacial stage, followed by aeolian deposition during a glacial stage. Repeated interglacial–glacial depositional sequences are present in the K2 to K5 terrace systems (Fig. 14). The only exception to this ordering is the K4 terrace system, which includes evidence of an additional marine transgression-regression event (Fig. 14).

Features such as wave-cut platforms and tidal notches are preserved within the coastal aeolianites of the K4 and K5 terrace systems. Similar features do not seem to be preserved in the older terraces (K1 to K3), either because they were eroded or covered by younger terrace

deposits. However, wave-cut platforms are likely to have formed along the coast during each of the sea-level maxima (Pedoja et al., 2014).

10.3. Climatic and autocyclic influences

Climatic conditions during the Pleistocene varied greatly (Zachos et al., 2001; Siddall et al., 2006), in part related to the frequency and amplitude of glacially controlled cycles, that were modulated by astronomical forcing (Lambeck et al., 2002).

Some of the variations in depositional environment in the north-Cyprus terraces can best be explained by cyclical climatic change. The basal part of each terrace comprises shallow-marine facies, locally interbedded with fluvial facies, which are interpreted as representing warm, humid interglacial periods, with high precipitation. A similar interpretation has been made for comparable deposits in areas, including southeast Italy (Celma et al., 2015), southeast Iran (Kober et al., 2013), and the Italian Apennines (Wegmann and Pazzaglia, 2009).

Erosion and sedimentation rates within the fluvial drainage systems of the K2 to K5 terrace systems were largely controlled by changes in climate during the Pleistocene glacial cycles. Pleistocene glacial cycles have been shown to affect fluvial systems elsewhere through climatically induced base-level changes that resulted in changes in sediment supply and erosion (Harvey, 2002). The fluvial drainage catchments identified within each of the Kyrenia Range terrace systems are likely to have responded differently to various allocyclic controls (see Candy et al., 2004) and require more focused study. Increased fluvial sedimentation is likely to be associated with interglacial periods because there is evidence of deltaic deposition during MIS 5e, which is therefore likely to represent a relatively wet climate period.

The stacked palaeosols within the basal parts of the K2 and K4 fluvial terrace deposits can be interpreted as representing periods of low fluvial runoff due to low precipitation. Similar interpretations apply to other fluvial sequences, for example, in the Vera Basin, SE Spain (Stokes and Mather, 2000).

Marine faunal assemblages, similar to those preserved within the marine deposits of the K4 terrace system, have been used to interpret climatic conditions during interglacial periods. The basal-marine conglomerates of the K4 terrace system contain the mollusc *Spondylus* and the coral *Cladocora*, both indicative of relatively warm-water conditions (Pedley and Grasso, 2002). *Cladocora* from the K4 terrace system has been dated at 243 ka (Palamakumbura et al., 2016b), equivalent to interglacial marine isotope stage 7. The above interpretations are in agreement with $^{18}O/^{16}O$ ratios analyzed from speleothem overgrowths in Mallorca, Spain (Vesica et al., 2000) and also in Israel (Bar-Matthews et al., 2000), suggesting warm climate conditions during MIS 7. Warm-water molluscs within the basal marine deposits of the K4 terrace system along the northern coast of the Kyrenia Range have been interpreted as representing MIS 7 (Galili et al., 2015). Dated corals representing a marine transgression within the K4 terrace system are correlated with the interglacial substage MIS 5e (Palamakumbura et al., 2016b). MIS 5e is interpreted to represent warm-water conditions, with initial coastal erosion followed by coastal deposition, based on data from Mallorca (Rose et al., 1999). Similar inferences apply to the northern coast of Cyprus, where a major terrace step is likely to have formed during MIS 5e between the K4 and K5 terrace systems.

The upper parts of all of the terrace systems are dominated by aeolian dune deposits, which are interpreted as representing relatively dry and cool climatic conditions during glacial periods. OSL dating in Mallorca has shown that aeolian deposition dominated during glacial stages MIS 5, 4, and 3 (Fornós et al., 2009), which is compatible with the available dating of the aeolianites of the K5 terrace system in northern Cyprus (Palamakumbura et al., 2016b).

Taking into account the interaction of the allocyclic controls on deposition, i.e., tectonics, eustatic sea-level change and climatic change, some facies variation may instead be better explained by autocyclic controls (Cecil, 2003). An example is the fluvial facies preserved within each terrace system and its hinterland, as represented by the numerous drainage catchments that record a wide range of fluvial processes. Deposits that range from high-energy debris-flow deposits to perennial stream deposits may in large part be explained by prevailing weather conditions.

11. Conclusions

Field-based facies evidence provides a basis for understanding the controls of deposition of a flight of Pleistocene marine and non-marine terrace systems exposed in the Kyrenia Range, northern Cyprus.

1. Six terrace depositional systems are defined and correlated along the northern and southern flanks of the Kyrenia Range (K0 to K5 terrace systems).
2. The oldest deposits within the uplifted terraces are lacustrine (lower part of K0 terrace system). The upper parts of the lacustrine deposits are interbedded with megabreccias indicating that lacustrine and slope wasting took place contemporaneously.
3. The upper part of the K0 terrace system comprises slope-talus megabreccias and debris-flow deposits. The K0 terrace system is interpreted as the product of extensive mass wasting of previously fault-fragmented Mesozoic metacarbonate rocks related to rapid surface uplift of the Kyrenia Range.
4. The K1 to K5 terrace systems comprise cycles of marine and non-marine facies on the northern flank of the range. Contemporaneous fluvial terraces developed on the southern flank of the range.
5. The K2 to K5 terrace systems on the northern range flank document marine transgressions followed by marine regressions. As an exception, the K4 terrace system has facies evidence of a second, short-lived marine transgression.
6. The basal-marine deposits are overlain and cut by channelized fluvial drainage catchments. Narrow, steep-sided channels were mainly filled by high-energy, mass-flow deposits, whereas wider and shallower channels show more evidence of traction current influence and perennial stream flow. Small Gilbert-type deltas formed locally along the coast within the K4 terrace system.
7. Aeolian dune fields formed at a late stage in each of the marine to non-marine cycles. The sediment was mostly derived from shallow-marine bioclastic material, coupled with the reworking of pre-existing aeolianite.
8. The basal marine and fluvial deposits of each terrace system can be correlated with global eustatic sea-level maxima during interglacial periods. In contrast, the aeolian carbonate deposits generally correlate with global sea-level minima during glacial periods.
9. Surface uplift of the Kyrenia Range began in the early Pleistocene climaxed in the early–mid Pleistocene and then waned in the mid-late Pleistocene to Recent.

References

Anastasakis, G., Kelling, G., 1991. Tectonic connection of the Hellenic and Cyprus arcs and related geotectonic elements. Marine Geology 97, 261–277.

Andreucci, S., Panzeri, L., Martini, I.P., Maspero, F., Martini, M., Pascucci, V., 2014. Evolution and architecture of a west Mediterranean upper Pleistocene to Holocene coastal apron-fan system. Sedimentology 61, 333–361.

Andreucci, S., Pascucci, V., Murray, A.S., Clemmensen, L.B., 2009. Late Pleistocene coastal evolution of San Giovanni di Sinis, west Sardinia (Western Mediterranean). Sedimentary Geology 216, 104–116.

Arakel, A.V., 1982. Genesis of calcrete in Quaternary soil profiles, Hutt and Leeman Lagoons, Western Australia. Journal of Sedimentary Research 52, 109–125.

Barka, A., Reilinger, R., 1997. Active tectonics of the Eastern Mediterranean region: deduced from GPS, neotectonic and seismicity data. Annali di Geofisica 11, 587–610.

Bar-Matthews, M., Ayalon, A., Kaufman, A., 2000. Timing and hydrological conditions of sapropel events in the Eastern Mediterranean, as evident from speleothems, Soreq Cave, Israel. Chemical Geology 169, 145–156.

Baroz, F., 1979. Etude géologique dans le Pentadaktylos et la Mesaoria (Chypre Septentrionale). Université de Nancy (Doctor of Science Thesis (published)).

Basilone, L., 2009. Mesozoic tectono-sedimentary evolution of Rocca Busambra in western Sicily. Facies 55, 115–135.

Blair, T.C., McPherson, J.G., 1999. Grain-size and textural classification of coarse sedimentary particles. Journal of Sedimentary Research 69, 6–19.

Blum, M.D., Törnqvist, T.E., 2000. Fluvial responses to climate and sea-level change: a review and look forward. Sedimentology 47, 2–48.

Bourgeois, J., Leithold, E.L., 1984. Wave-worked conglomerates-depositional processes and criteria for recognition. In: Koster, E.H., Steel, R.J. (Eds.), Sedimentology of Gravels and Conglomerates. Canadian Society of Petroleum Geologists, Memoir 10, pp. 331–343.

Bridgland, D., Westaway, R., 2008. Climatically controlled river terrace staircases: a worldwide Quaternary phenomenon. Geomorphology 98, 285–315.

Brooke, B., 2001. The distribution of carbonate eolianite. Earth-Science Reviews 55, 135–164.

Buchbinder, B., Zilberman, E., 1997. Sequence stratigraphy of Miocene–Pliocene carbonate-siliciclastic shelf deposits in the eastern Mediterranean margin (Israel): effects of eustasy and tectonics. Sedimentary Geology 112, 7–32.

Burchette, T.P., Wright, V.P., 1992. Carbonate ramp depositional systems. Sedimentary Geology 79, 3–57.

Calon, T.J., Aksu, A.E., Hall, J., 2005. The Oligocene—recent evolution of the Mesaoria Basin (Cyprus) and its western marine extension, Eastern Mediterranean. Marine Geology 221, 95–120.

Candy, I., Black, S., 2009. The timing of Quaternary calcrete development in semi-arid southeast Spain: investigating the role of climate on calcrete genesis. Sedimentary Geology 220, 6–15.

Candy, I., Black, S., Sellwood, B.W., 2004. Interpreting the response of a dryland river system to Late Quaternary climate change. Quaternary Science Reviews 23, 2513–2523.

Cavinato, G.P., Carusi, C., Dall'asta, M., Miccadei, E., Piacentini, T., 2002. Sedimentary and tectonic evolution of Plio-Pleistocene alluvial and lacustrine deposits of Fucino Basin (central Italy). Sedimentary Geology 148, 29–59.

Cecil, C., 2003. The concept of autocyclic and allocyclic controls on sedimentation and stratigraphy, emphasizing the climatic variable. In: Cecil, C.B., Edgar, T.N. (Eds.), Climate Controls on Stratigraphy. SEPM Special Publication 77, pp. 13–20.

Celma, D.C., Pieruccini, P., Farabollini, P., 2015. Major controls on architecture, sequence stratigraphy and paleosols of Middle Pleistocene continental sediments ("Qc Unit"), eastern central Italy. Quaternary Research 83, 565–581.

Clift, P.D., 2006. Controls on the erosion of Cenozoic Asia and the flux of clastic sediment to the ocean. Earth and Planetary Science Letters 241, 571–580.

Clifton, H.E., Hunter, R.E., Phillips, R.L., 1973. Structures and processes in the non-barred high energy nearshore. Journal of Sedimentary Petrology 41, 651–670.

Cornée, J.J., Léticée, J.L., Münch, P., Quillévéré, F., Lebrun, J.F., Moissette, P., Braga, J.C., Melinte-Dobrinescu, M., De Min, L., Oudet, J., Randrianasolo, A., 2012. Sedimentology, palaeoenvironments and biostratigraphy of the Pliocene-Pleistocene carbonate platform of Grande-Terre (Guadeloupe, Lesser Antilles forearc). Sedimentology 59, 1426–1451.

Coussot, P., Meunier, M., 1996. Recognition, classification and mechanical description of debris flows. Earth-Science Reviews 40, 209–227.

Dodonov, A.E., Trifonov, V.G., Ivanova, T.P., Kuznetsov, V.Y., Maksimov, F.E., Bachmanov, D.M., Sadchikova, T.A., Simakova, A.N., Minini, H., Al-Kafri, A.-M., Ali, O., 2008. Late Quaternary marine terraces in the Mediterranean coastal area of Syria: geochronology and neotectonics. Quaternary International 190, 158–170.

Dreghorn, W., 1978. Landforms in the Girne Range Northern Cyprus. Ankara, Maden Tetkik we Arama Enstitüsü, Ankara.

Ducloz, C., 1964. Geological Map of the Central Kyrenia Range. Geological Survey Department, Government of Cyprus.

Ducloz, C., 1965. Revision of the Pliocene and Quaternary stratigraphy of the central Mesaoria, Nicosia. Annual Report of the Geological Survey Department Cyprus 31–42.

Ducloz, C., 1972. The geology of the Bellapais–Kythrea area of the Central Kyrenia Range. Bulletin of the Geological Survey Department 6, 44–71.

Elmejdoub, N., Jedoui, Y., 2009. Pleistocene raised marine deposits of the Cap Bon Peninsula (N–E Tunisia): records of sea-level highstands, climatic changes and coastal uplift. Geomorphology 112, 179–189.

Erginal, A.E., Kiyak, N.G., Ertek, T.A., 2012. A new Late Holocene eolianite record from Altınkum beach, North Cyprus. Turkish Journal of Earth Sciences 21, 407–414.

Fabbricatore, D., Robustelli, G., Muto, F., 2014. Facies analysis and depositional architecture of shelf-type deltas in the Crati Basin (Calabrian Arc, south Italy). Italian Journal of Geosciences 133, 131–148.

Fernandes, R.M.S., 2003. The relative motion between Africa and Eurasia as derived from ITRF2000 and GPS data. Geophysical Research Letters 30, 1–5. http://dx.doi.org/10.1029/2003GL017089.

Ferranti, L., Antonioli, F., Mauz, B., Amorosi, A., Dai Pra, G., Mastronuzzi, G., Monaco, C., Orrù, P., Pappalardo, M., Radtke, U., Renda, P., Romano, P., Sansò, P., Verrubbi, V., 2006. Markers of the last interglacial sea-level high stand along the coast of Italy: tectonic implications. Quaternary International 145–146, 30–54.

Ford, D., Golonka, J., 2003. Phanerozoic paleogeography, paleoenvironment and lithofacies maps of the circum-Atlantic margins. Marine and Petroleum Geology 20, 248–285.

Fornós, J.J., Clemmensen, L.B., Gómez-Pujol, L., Murray, A.S., 2009. Late Pleistocene carbonate aeolianites on Mallorca, Western Mediterranean: a luminescence chronology. Quaternary Science Reviews 28, 2697–2709.

Frébourg, G., Hasler, C.-A., Le Guern, P., Davaud, E., 2008. Facies characteristics and diversity in carbonate eolianites. Facies 54, 175–191.

Frechen, M., Neber, A., Tsatskin, A., Boenigk, W., Ronen, A., 2004. Chronology of Pleistocene sedimentary cycles in the Carmel coastal plain of Israel. Quaternary International 121, 41–52.

Galili, E., Şevketoğlu, M., Salamon, A., Zviely, D., Mienis, H., Rosen, B., Moshkovitz, S., 2015. Late Quaternary beach deposits and archaeological relicts on the coasts of Cyprus, and the possible implications of sea-level changes and tectonics on the early populations. In: Harff, J., Bailey, G., Lüth, F. (Eds.), Geology and Archaeology: Submerged Landscapes of the Continental Shelf. Geological Society of London, Special Publications 411, pp. 179–218.

Ghinassi, M., Magi, M., Sagri, M., Singer, B.S., 2004. Arid climate 2.5 Ma in the Plio-Pleistocene Valdarno Basin (Northern Apennines, Italy). Palaeogeography, Palaeoclimatology, Palaeoecology 207, 37–57.

Gross, M., 1964. Variations in the O^{18}/O^{16} and C^{13}/C^{12} ratios of diagenetically altered limestones in the Bermuda Islands. Journal of Geology 72, 170–194.

Hakyemez, Y., Turhan, N., Sönmez, I., Sümengen, M., 2000. Kuzey Kıbrıs Turk Cumhuriyeti'nin Jeolojisi (Geology of the Turkish Republic of Northern Cyprus), Unpublished report of MTA (Maden Tektik ve Arama), Genel Mudurlugu Jeoloji Etutleri Diaresi, Ankara.

Hall, R., Nichols, G., 2002. Cenozoic sedimentation and tectonics in Borneo: climatic influences on orogenesis. In: Jones, S.J., Frostick, L.E. (Eds.), Sediment Flux to Basins: Causes, Controls and Consequences. Geological Society of London, Special Publications 191, pp. 5–22.

Hansen, K.S., 1999. Development of a prograding carbonate wedge during sea level fall: lower Pleistocene of Rhodes, Greece. Sedimentology 46, 559–576.

Harrison, R., Newell, W., Panayides, I., Stone, B., Tsiolakis, E., Necdet, M., Batihanli, H., Ozhur, A., Lord, A., Berksoy, O., Zomeni, Z., Schindler, J.S., U.S.G.S., 2008. Bedrock Geologic Map of the Greater Lefkosia Area, Cyprus. US Geological Survey, Reston, Virginia.

Harrison, R.W., Tsiolakis, E., Stone, B.D., Lord, A., Mcgeehin, J.P., Mahan, S.A., Chirico, P., 2012. Late Pleistocene and Holocene uplift history of Cyprus: implications for active tectonics along the southern margin of the Anatolian microplate. In: Robertson, A.H.F., Parlak, O., Ünlügenç, U.C. (Eds.), Geological Development of Anatolia and the Easternmost Mediterranean Region. Geological Society of London, Special Publications 372, pp. 561–584.

Harvey, A.M., 2002. The role of base-level change in the dissection of alluvial fans: case studies from southeast Spain and Nevada. Geomorphology 45, 67–87.

Hearty, P.J., O'Leary, M.J., 2008. Carbonate eolianites, quartz sands, and Quaternary sea-level cycles, Western Australia: a chronostratigraphic approach. Quaternary Geochronology 3, 26–55.

Hudson, J.D., 1977. Stable isotopes and limestone lithification. Journal of the Geological Society 133, 637–660.

Kasse, C.K., 2002. Sandy aeolian deposits and environments and their relation to climate during the Last Glacial Maximum and Lateglacial in northwest and central Europe. Progress in Physical Geography 26, 507–532.

Kempler, D., Ben-Avraham, Z., 1987. The tectonic evolution of the Cyprean Arc. Annales Tectonicae 1, 58–71.

Kindler, P., Mazzolini, D., 2001. Sedimentology and petrography of dredged carbonate sands from Stocking Island (Bahamas). Implications for meteoric diagenesis and aeolianite formation. Palaeogeography, Palaeoclimatology, Palaeoecology 175, 369–379.

Knup, P.E., 1965. Geological Map of the Central Kyrenia Range. Cyprus Geological Survey Department, Nicosia.

Kober, F., Zeilinger, G., Ivy-Ochs, S., Dolati, A., Smit, J., Kubik, P.W., 2013. Climatic and tectonic control on fluvial and alluvial fan sequence formation in the Central Makran Range, SE-Iran. Global and Planetary Change 111, 133–149.

Kourampas, A., Robertson, A.H.F., 2000. Controls on Plio-Quaternary sedimentation within an active fore-arc region: Messenia Peninsula (SW Peloponnese), S. Greece. In: Panayides, I., Xenophonotos, C., Malpas, J. (Eds.), Proceedings of the Third International Conference on the Geology of the Eastern Mediterranean 2000. Cyprus Geological Survey Department, Nicosia Cyprus, pp. 255–285.

Kraus, M.J., 1999. Paleosols in clastic sedimentary rocks: their geologic applications. Earth-Science Reviews 47, 41–70.

Kumar, R., Ghosh, S.K., Mazari, R., Sangode, S., 2003. Tectonic impact on the fluvial deposits of Plio-Pleistocene Himalayan foreland basin, India. Sedimentary Geology 158, 209–234.

Lakhdar, R., Soussi, M., Ben Ismail, M.H., M'Rabet, A., 2006. A Mediterranean Holocene restricted coastal lagoon under arid climate: case of the sedimentary record of Sabkha Boujmel (SE Tunisia). Palaeogeography, Palaeoclimatology, Palaeoecology 241, 177–191.

Lambeck, K., Esat, T.M., Potter, E., 2002. Links between climate and sea levels for the past three million years. Nature 419, 199–206.

Leeder, M.R., Seger, M.J., Stark, C.P., 1991. Sedimentation and tectonic geomorphology adjacent to major active and inactive faults, southern Greece. Journal of the Geological Society 148, 331–343.

Lemons, D.R., Chan, M.A., 1999. Facies architecture and sequence stratigraphy of fine-grained lacustrine deltas along the eastern margin of late Pleistocene Lake Bonneville, Northern Utah and Southern Idaho. American Association of Petroleum Geologists Bulletin 83, 635–665.

Macklin, M.G., Fuller, I.C., Lewin, J., Maas, G.S., Passmore, D.G., Rose, J., Woodward, J.C., Black, S., Hamlin, R.H.B., Rowan, J.S., 2002. Correlation of fluvial sequences in the Mediterranean basin over the last 200 ka and their relationship to climate change. Quaternary Science Reviews 21, 1633–1641.

Maddy, D., Demir, T., Bridgland, D.R., Veldkamp, A., Stemerdink, C., van der Schriek, T., Westaway, R., 2008. The Early Pleistocene development of the Gediz River, Western Turkey: an uplift-driven, climate-controlled system? Quaternary International 189, 115–128.

Main, C.E., Robertson, A.H.F., Palamakumbura, R.N., 2016. Pleistocene geomorphological and sedimentary development of the Akaki River catchment (northeastern Troodos Massif) in relation to tectonic uplift versus climatic change. International Journal of Earth Sciences 105, 463–485.

Mauz, B., Vacchi, M., Green, A., Hoffmann, G., Cooper, A., 2015. Beachrock: a tool for reconstructing relative sea level in the far-field. Marine Geology 362, 1–16.

McCay, G., Robertson, A.H.F., 2012a. Late Eocene–Neogene sedimentary geology of the Girne (Kyrenia) Range, northern Cyprus: a case history of sedimentation related to progressive and diachronous continental collision. Sedimentary Geology 265-266, 30–55.

McCay, G., Robertson, A.H.F., 2012b. Upper Miocene–Pleistocene deformation of the Girne (Kyrenia) Range and Dar Dere (Ovgos) lineament, northern Cyprus: role in collision and tectonic escape in the easternmost Mediterranean region. In: Robertson, A.H.F., Parlak, O., Ünlügenç, U.C. (Eds.), Geological Development of Anatolia and the Easternmost Mediterranean Region. Geological Society of London Special Publication 372, pp. 421–445.

McCay, G., Robertson, A.H.F., Kroon, D., Raffi, I., Ellam, R.M., Necdet, M., 2012. Stratigraphy of Cretaceous to Lower Pliocene sediments in the northern part of Cyprus based on comparative $^{87}Sr/^{86}Sr$ isotopic, nannofossil and planktonic foraminiferal dating. Geological Magazine 150, 333–359.

McClusky, S., Reilinger, R., Mahmoud, S., Ben Sari, D., Tealeb, A., 2003. GPS constraints on Africa (Nubia) and Arabia plate motions. Geophysical Journal International 155, 126–138.

McLaren, S.J., 1993. Use of cement types in the palaeoenvironmental interpretation of coastal aeolianite sequences. In: Pye, K. (Ed.), The Dynamics and Environmental Context of Aeolian Sedimentary Systems. Geological Society of London Special Publications 72, pp. 235–244.

Mosbrugger, V., Utescher, T., Dilcher, D.L., 2005. Cenozoic continental climatic evolution of Central Europe. Proceedings of the National Academy of Sciences of the United States of America 102, 14964–14969.

Nelson, C.S., Smith, A.M., 1996. Stable oxygen and carbon isotope compositional fields for skeletal and diagenetic components in New Zealand Cenozoic nontropical carbonate sediments and limestones: a synthesis and review. New Zealand Journal of Geology and Geophysics 39, 93–107.

Nemec, W., Kazanci, N., 1999. Quaternary colluvium in west-central Anatolia: Sedimentary facies and palaeoclimatic significance. Sedimentology 46, 139–170.

Nielsen, K.A., Clemmensen, L.B., Fornós, J.J., 2004. Middle Pleistocene magnetostratigraphy and susceptibility stratigraphy: data from a carbonate aeolian system, Mallorca, Western Mediterranean. Quaternary Science Reviews 23, 1733–1756.

Öztürk, B., Buzzurro, G., Benli, H.A., 2003. Marine molluscs from Cyprus: new data and checklist. Bolleffino Malacologico 39, 49–78.

Palamakumbura, R.N., 2015. Sedimentary response to the tectonic uplift of the Kyrenia Range, northern Cyprus, in its Eastern Mediterranean tectonic setting. Unpublished PhD thesis, University of Edinburgh.

Palamakumbura, R.N., Robertson, A.H.F., Kinnaird, T.C., Sanderson, D.C.W., 2016a. Sedimentary development and correlation of Late Quaternary terraces in the Kyrenia Range, northern Cyprus, using a combination of sedimentology and optical luminescence data. International Journal of Earth Sciences 105, 463–485.

Palamakumbura, R.N., Robertson, A.H.F., Kinnaird, T.C., Van Calsteren, P., Kroon, D., Tait, J., 2016b. Quantitative dating of Pleistocene deposits of the Kyrenia Range, northern Cyprus: implications for timings, rates of uplift and driving mechanisms. Journal of the Geological Society (in press).

Pedley, M., Carannante, G., 2006. Cool-water carbonate ramps: a review. In: Pedley, H.M., Carannante, G. (Eds.), Cool-Water Carbonates: Depositional Systems and Palaeoenvironmental Controls. Geological Society of London, Special Publications 255, pp. 1–9.

Pedley, M., Grasso, M., 2002. Lithofacies modelling and sequence stratigraphy in microtidal cool-water carbonates: a case study from the Pleistocene of Sicily, Italy. Sedimentology 49, 533–553.

Pedoja, K., Husson, L., Johnson, M.E., Melnick, D., Witt, C., Pochat, S., Nexer, M., Delcaillau, B., Pinegina, T., Poprawski, Y., Authemayou, C., Elliot, M., Regard, V., Garestier, F., 2014. Coastal staircase sequences reflecting sea-level oscillations and tectonic uplift during the Quaternary and Neogene. Earth-Science Reviews 132, 13–38.

Poole, A., Robertson, A., 1998. Pleistocene fanglomerate deposition related to uplift of the Troodos Ophiolite, Cyprus. In: Robertson, A.H.F., Emeis, K., Richter, C. (Eds.), Proceedings of the Ocean Drilling Program. Scientific Results 160, pp. 545–566.

Poole, A.J., Robertson, A.H.F., 2000. Quaternary marine terrace and aeolianites in coastal south and west Cyprus: implications for regional uplift and sea-level change. In:

Panayides, I., Xenophontos, C., Malpas, J. (Eds.), Proceedings of the Third International Conference on the Geology of the Eastern Mediterranean. Geological Survey Department, Ministry of Agriculture and Natural Resources, pp. 105–123.

Quigley, M.C., Sandiford, M., Cupper, M.L., 2007. Distinguishing tectonic from climatic controls on range-front sedimentation. Basin Research 19, 491–505.

Reyss, J.L., Pirazzoli, P.A., Haghipour, A., Hatte, C., Fontugne, M., 1998. Quaternary marine terraces and tectonic uplift rates on the south coast of Iran. In: Reyss, J., Pirazzoli, P.A., Haghipour, A. (Eds.), Coastal Tectonics. Geological Society of London, Special Publications 146, pp. 225–237.

Robertson, A.H.F., Kinnaird, T.C., 2016. Structural development of the central Kyrenia Range (north Cyprus) in its regional setting in the eastern Mediterranean region. International Journal of Earth Sciences 105, 417–437.

Robertson, A.H.F., Woodcock, N.H., 1986. The role of the Kyrenia Range lineament, Cyprus, in the geological evolution of the Eastern Mediterranean area. In: Reading, H.G., Watterson, J., White, S.H. (Eds.), Major Crustal Lineaments and Their Influences on the Geological History of Continental Lithosphere. Philosophical Transactions of the Royal Society A: Mathematical, Physical and Engineering Sciences 317, pp. 141–177.

Robertson, A.H.F., McCay, G.A., Taslı, K., Yıldız, A., 2014. Eocene development of the northerly active continental margin of the Southern Neotethys in the Kyrenia Range, north Cyprus. Geological Magazine 151, 692–731.

Robertson, A.H.F., Parlak, O., Ustaömer, T., 2012. Overview of the Palaeozoic–Neogene evolution of Neotethys in the Eastern Mediterranean region (southern Turkey, Cyprus, Syria). Petroleum Geoscience 18, 381–404.

Rohais, S., Eschard, R., Ford, M., Guillocheau, F., Moretti, I., 2007. Stratigraphic architecture of the Plio-Pleistocene infill of the Corinth Rift: implications for its structural evolution. Tectonophysics 440, 5–28.

Rose, J., Meng, X., Watson, C., 1999. Palaeoclimate and palaeoenvironmental responses in the western Mediterranean over the last 140 ka: evidence from Mallorca, Spain. Journal of the Geological Society 156, 435–448.

Sanders, D., Ostermann, M., Kramers, J., 2009. Quaternary carbonate-rocky talus slope successions (Eastern Alps, Austria): sedimentary facies and facies architecture. Facies 55, 345–373.

Schirmer, W., 1998. Havara on Cyprus—a surficial calcareous deposit. Eiszeitalter und Gegenwart 48, 110–117.

Siddall, M., Chappell, J., Potter, E., 2006. Eustatic sea level during past interglacials. Developments in Quaternary Sciences 7, 75–92.

Starkel, L., 2003. Climatically controlled terraces in uplifting mountain areas. Quaternary Science Reviews 22, 2189–2198.

Stewart, I.S., Hancock, P.L., 1990. Brecciation and fracturing within neotectonic normal fault zones in the Aegean region. In: Knipe, R.J., Rutter, E.H. (Eds.), Deformation Mechanisms, Rheology and Tectonics. Geological Society of London, Special Publications 54, pp. 105–110.

Stokes, M., Mather, A.E., 2000. Response of Plio-Pleistocene alluvial systems to tectonically induced base-level changes, Vera Basin, SE Spain. Journal of the Geological Society 157, 303–316.

Thomas, J.V., Parkash, B., Mohindra, R., 2002. Lithofacies and palaeosol analysis of the Middle and Upper Siwalik Groups (Plio-Pleistocene), Haripur-Kolar section, Himachal Pradesh, India. Sedimentary Geology 150, 343–366.

Titschack, J., Bromley, R.G., Freiwald, A., 2005. Plio-Pleistocene cliff-bound, wedge-shaped, warm-temperate carbonate deposits from Rhodes (Greece): sedimentology and facies. Sedimentary Geology 180, 29–56.

Trauth, M.H., Larrasoaña, J.C., Mudelsee, M., 2009. Trends, rhythms and events in Plio-Pleistocene African climate. Quaternary Science Reviews 28, 399–411.

Vesica, P.L., Tuccimei, P., Turi, B., Fornós, J.J., Ginés, A., Ginés, J., 2000. Late Pleistocene Paleoclimates and sea-level change in the Mediterranean as inferred from stable isotope and U-series studies of overgrowths on speleothems, Mallorca, Spain. Quaternary Science Reviews 19, 865–879.

Waters, J.V., Jones, S.J., Armstrong, H.A., 2010. Climatic controls on Late Pleistocene alluvial fans, Cyprus. Geomorphology 115, 228–251.

Wegmann, K.W., Pazzaglia, F.J., 2009. Late Quaternary fluvial terraces of the Romagna and Marche Apennines, Italy: climatic, lithologic, and tectonic controls on terrace genesis in an active orogen. Quaternary Science Reviews 28, 137–165.

Weiler, Y., 1970. Mode of occurrence of pelites in the Kythrea Flysch basin (Cyprus). Journal of Sedimentary Research 40, 1255–1261.

Welford, J.K., Hall, J., Christian, H., Louden, K., 2015. Crustal seismic velocity structure from Eratosthenes Seamount to Hecataeus Rise across the Cyprus Arc, eastern Mediterranean. Geophysical Journal International 200, 933–951.

Wentworth, C.K., 1922. A scale of grade and class terms for clastic sediments. Journal of Geology 30, 377–392.

Westaway, R., Bridgland, D., 2007. Late Cenozoic uplift of southern Italy deduced from fluvial and marine sediments: coupling between surface processes and lower-crustal flow. Quaternary International 175, 86–124.

Zachos, J., Pagani, M., Sloan, L., Thomas, E., Billups, K., 2001. Trends, rhythms, and aberrations in global climate 65 Ma to present. Science 292, 686–693.

Zazo, C., Goy, J.L., Dabrio, C.J., Bardají, T., Hillair-Marcel, C., Ghaleb, B., González-Delgado, J.-Á., Soler, V., 2003. Pleistocene raised marine terraces of the Spanish Mediterranean and Atlantic coasts: records of coastal uplift, sea-level highstands and climate changes. Marine Geology 194, 103–133.

Zecchin, M., Nalin, R., Roda, C., 2004. Raised Pleistocene marine terraces of the Crotone peninsula (Calabria, southern Italy): facies analysis and organization of their deposits. Sedimentary Geology 172, 165–185.